Cell Reports
Medicine

Article

CD97-directed CAR-T cells with enhanced persistence eradicate acute myeloid leukemia in diverse xenograft models

Graphical abstract

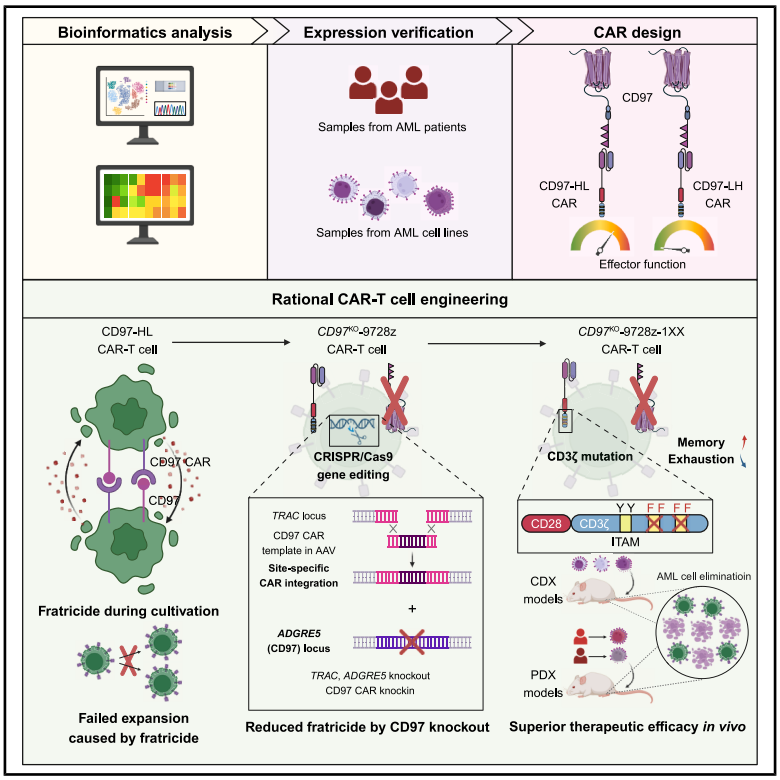

Highlights

- CD97 is a suitable target for CAR-T therapy against AML
- CD97 knockout strategy mitigated the fratricide on CD97-targeting CAR-T cells
- *CD97*^{KO} CAR-T cells showed tolerable cytotoxicity to HSPCs
- *CD97*^{KO}-9728z-1XX CAR-T cells displayed superior functions both *in vitro* and *in vivo*

Authors

Kai Shang, Deyu Huang, Jun Liu, ..., Shanshan Pei, Pengxu Qian, Jie Sun

Correspondence

huanghe@zju.edu.cn (H.H.), shanshan.pei@zju.edu.cn (S.P.), axu@zju.edu.cn (P.Q.), sunj4@zju.edu.cn (J.S.)

In brief

Shang et al. demonstrate that CD97 is a promising target for CAR-T therapy against AML. CD97 knockout can resolve the fratricide problem caused by CD97 expression on T cells. Optimized *CD97*^{KO}-9728z-1XX CAR-T cells showed persistent anti-tumor activity in both CDX models and PDX models.

Shang et al., 2025, Cell Reports Medicine 6, 102148
June 17, 2025
https://doi.org/10.1016/j.xcrm.2025.102148

CellPress

Cell Reports Medicine

CellPress
OPEN ACCESS

Article

CD97-directed CAR-T cells with enhanced persistence eradicate acute myeloid leukemia in diverse xenograft models

Kai Shang,[1,2,3,4,5,12] Deyu Huang,[1,2,4,5,6,12] Jun Liu,[2,7,12] Zebin Yu,[1,2,4,5,6] Wei Bian,[2] Jiangqing Chen,[1,2,3,4,5] Yin Zhao,[2] Lina Liu,[1] Jie Jiang,[1,2,3,4,5] Yajie Wang,[1,2,3,4,5] Yanting Duan,[1,2,3,4,5,11] Jingyu Ge,[8] Shize Zhang,[9] Chun Zhou,[10] Yingli Han,[1,2,4,5,6] Yongxian Hu,[1,2,4] Weiyan Zheng,[1] Jie Sun,[1] He Huang,[1,2,4,5,*] Shanshan Pei,[1,2,4,*] Pengxu Qian,[1,2,4,5,6,*] and Jie Sun[1,2,3,4,5,13,*]

[1]Bone Marrow Transplantation Center of the First Affiliated Hospital, Zhejiang University School of Medicine, 866 Yuhangtang Road, Hangzhou 310058, China
[2]Liangzhu Laboratory, Zhejiang University, 1369 West Wenyi Road, Hangzhou 311121, China
[3]Department of Cell Biology, Zhejiang University School of Medicine, 866 Yuhangtang Road, Hangzhou 310058, China
[4]Institute of Hematology, Zhejiang University, Hangzhou 310058, China
[5]Zhejiang Province Engineering Laboratory for Stem Cell and Immunity Therapy, Hangzhou 310058, China
[6]Center for Stem Cell and Regenerative Medicine, Zhejiang University School of Medicine, Hangzhou 310058, China
[7]Zhejiang University School of Medicine, 866 Yuhangtang Road, Hangzhou 310058, China
[8]Department of Medical Oncology, The First Affiliated Hospital, Zhejiang University School of Medicine, Hangzhou 310003, China
[9]Center for Genetic Medicine, The Fourth Affiliated Hospital, Zhejiang University School of Medicine, Hangzhou 310058, China
[10]School of Public Health, Zhejiang University School of Medicine, 866 Yuhangtang Road, Hangzhou 310058, China
[11]Present address: Zhejiang Key Laboratory of Precision Medicine Research on Head & Neck Cancer, Hangzhou 310014, China
[12]These authors contributed equally
[13]Lead contact
*Correspondence: huanghe@zju.edu.cn (H.H.), shanshan.pei@zju.edu.cn (S.P.), axu@zju.edu.cn (P.Q.), sunj4@zju.edu.cn (J.S.)
https://doi.org/10.1016/j.xcrm.2025.102148

SUMMARY

Chimeric antigen receptor (CAR)-T therapy on acute myeloid leukemia (AML) is hindered by the absence of a suitable tumor-specific antigen. Here, we propose CD97 as a potential target for CAR-T therapy against AML based on its broader and higher expression on AML cells compared to normal hematopoietic stem and progenitor cells (HSPCs). To resolve the fratricide problem caused by CD97 expression on T cells, we knock out CD97 in CAR-T cells using CRISPR-Cas9. Our *CD97*^{KO} CAR-T cells eliminate both AML cell lines and primary AML cells effectively while showing tolerable toxicity to HSPCs. Furthermore, we mutate the CD3ζ domain of the CAR and find that the optimized CD97 CAR-T cells exhibit persistent anti-tumor activity both *in vitro* and in multiple xenograft models. Mechanistically, transcriptional profiles reveal that the optimized CAR-T cells delay differentiation and resist exhaustion. Collectively, our study supports CD97 as a promising target for CAR-T therapy against AML.

INTRODUCTION

Acute myeloid leukemia (AML) is a prevalent acute leukemia in adults, characterized by the blocked differentiation and abnormal proliferation of immature myeloid cells, leading to hematopoietic disorder and life-threatening cytopenia. The incidence rate of AML tends to increase gradually with age, along with a decline in overall survival. For example, over two-thirds of AML diagnoses occurred in patients older than 55 years. Meanwhile, for patients under 65, the overall survival rate is approximately 40%–45%, while, for those older than 65, it drops to only 10%–15%.[1–4] Standard treatments, such as 7 + 3 regimen[3] (cytarabine for 7 days and anthracycline for 3 days), had moderate changes over the past decades. More than half of patients experienced relapse within a year, and fewer than one-third of adult patients achieved durable remission.[5–7] The inherent heterogeneity of AML blasts,[8,9] coupled with the resistance of leukemia stem cells (LSCs) to chemotherapy,[10–12] presents a formidable obstacle to the effective treatment of AML.

Chimeric antigen receptor (CAR)-T cell therapy has made remarkable achievements[13,14] in treating refractory or relapsed B cell malignancies[15] and multiple myeloma.[16] However, the efficacy of CAR-T therapy in AML patients has fallen short of expectations. One major challenge is the absence of a lineage-specific target like CD19 in B cells. Most of the antigens expressed on AML blasts and LSCs are also expressed on normal cells, especially hematopoietic stem cells (HSCs). So far, CAR-T cells targeting antigens such as Lewis Y,[17] CD33,[18] CD123,[19] CD44v6,[20] CLL-1,[21] FLT-3,[22] CD70,[23] and Siglec-6[24] have shown some effectiveness in preclinical AML models. Among

these targets, CAR-T cells targeting CD33, CD123, and CLL-1 have been tested in clinical trials. However, few successful cases have been reported[25–27] due to the high heterogeneity of AML blasts. Besides, many of them could induce off-tumor toxicity to normal hematopoiesis due to the shared antigen expression on HSCs, resulting in granulocytopenia, anemia, thrombocytopenia, etc.[25,27–30]

CD97, encoded by *ADGRE5*, belongs to the adhesion G protein-coupled receptor (aGPCR) family. Numerous studies have highlighted the role of CD97 in promoting the invasion of various tumor cells, including those from colorectal,[31] thyroid,[32] liver,[33] gastric,[34] brain,[35] and prostatic cancer.[36] Previously, it has been demonstrated that CD97 is up-regulated in primary AML cells and LSCs compared to the normal bone marrow (BM) cells.[37–39] Notably, CD97 exhibits a minimal expression level in HSCs.[39,40] High CD97 expression in AML is also associated with poor survival.[40,41] Additionally, CD97 plays a crucial role in the proliferation and survival of AML blasts and LSCs, maintaining their undifferentiation state.[40] All these pieces of evidence suggest that CD97 could be a suitable target for AML treatment.

In this study, we evaluated the therapeutic efficacy of CAR-T cells targeting CD97 for AML treatment. Based on the second-generation CAR design, we proved that CD97 CAR-T cells could eliminate AML cells both *in vitro* and *in vivo*, with tolerable toxicity to hematopoietic stem and progenitor cells (HSPCs). Through optimization of the co-stimulatory and the activation domain, we found that a CAR design encoding a single immunoreceptor tyrosine-based activation motif (ITAM) exhibited sustained anti-tumor activity in both representative AML cell lines and patient-derived xenograft (PDX) models by balancing effector and memory programs. Our data support CD97 as a promising target for CAR-T therapy against AML.

RESULTS

CD97 is a suitable target for CAR-T therapy against AML

To assess the suitability of CD97 as a target against AML, we initially examined CD97 expression on BM cells in AML patients and healthy individuals using Gene Expression Profiling Interactive Analysis (GEPIA2)[42] and GEO[43] database. We found that CD97 was expressed at higher levels in AML blasts from patients compared to normal BM cells and HSCs from healthy individuals (Figures S1A and S1B). There was no significant difference of CD97 expression between $CD34^+$ LSCs and $CD34^-$ AML blasts, but both groups displayed much higher CD97 expression than normal $CD34^+$ HSPCs (Figure 1A). Kaplan-Meier analysis showed a strong correlation between high CD97 expression and poor survival (Figure S1C). Moreover, we observed consistently elevated CD97 expression across multiple karyotypes (1,793/1,800 above the average of HSCs, same below) using the BloodSpot database[44] (Figure 1B). In comparison to other targets against AML under clinical trials, targeting CD97 provides more extensive coverage than CD33 (1,680/1,800, Figure S1D), CD123 (1,662/1,800, Figure S1E), and CLL-1 (1,524/1,800, Figure S1F). Furthermore, we validated high CD97 expression on the surface of multiple AML cell lines belonging to different French-American-British (FAB) subtypes through immunoblotting (Figure S1G) and flow cytometry (Figure 1C). For primary AML cells derived from BM of 14 AML patients with diverse FAB subtypes and mutational profiles including *FLT-3* and *RAS* mutations that are often therapeutically resistant in the AML clinic, all specimens were CD97 positive (Figures 1D and S1H and Table S1). Collectively, these data suggest that CD97 is broadly and highly expressed in AML cell lines and primary AML specimens, and this elevated CD97 expression is associated with poor survival in the clinic, which is consistent with previous studies.[37–41] Thus, CD97 is a potential target for CAR-T therapy against AML.

Generation and characterization of CD97-targeting CAR-T cells

We generated a CAR construct with CD97-specific single-chain variable fragments (scFv) derived from a murine monoclonal antibody, followed by a CD28 hinge and transmembrane domain, CD28 co-stimulatory domain, and a CD3ζ activation domain. Enhanced green fluorescent protein (EGFP) was used as an indicator of CAR expression (Figure 2A). To account for the potential impacts of the variable heavy-chain (V_H) and variable light-chain (V_L) order on scFv properties and functions, we generated two CAR variants: CD97-HL and CD97-LH CARs (Figure 2A). Both CARs were successfully expressed in T cells transduced by retrovirus (Figure 2B). However, only CD97-HL CAR-T cells effectively killed various AML cell lines (Figure 2C) and produced effector cytokines tumor necrosis factor alpha (TNF-α) and interferon (IFN)-γ in an antigen-dependent way (Figures S2A–S2E). Therefore, we chose the scFv with the V_H-V_L order for the subsequent experiments.

CD97 is also expressed on the T cell surface, as indicated by the BloodSpot database (Figure 2D). Flow cytometry confirmed that CD97 was constitutively expressed on T cells and even up-regulated after stimulation by CD3/CD28 beads (Figure 2E), which was reproducible in multiple donors (Figure S2F). Thus CD97-targeting CAR-T cells may show fratricide effects. Indeed, 72 h after transduction, we observed a rapid decline in CAR-T cell viability (Figure 2F) and failure of expansion (Figures 2G and 2H). In contrast to CD97-HL CAR, CD97-LH CAR-T cells were spared from fratricide (Figures 2F–2H), consistent with their much lower effector functions (Figures 2C and S2A–S2D). Additionally, fratricide resulted in enrichment for CAR^+ T cells, explaining why the percentage of CD97-HL CAR^+ cells was much higher than that of CD97-LH CAR^+ cells (Figure 2B). Together, these findings demonstrated that CD97 expression on T cells caused severe fratricide in CD97-targeting CAR-T cells, requiring further refinement of the CAR-T construct.

CD97^{KO}-9728z CAR-T cells mitigated the fratricide and exerted both *in vitro* and *in vivo* anti-tumor efficacy

To alleviate fratricide, we employed CRISPR-Cas9 to knock out the CD97 encoding gene, *ADGRE5*. Among the limited single guide RNAs (sgRNAs) generated by the online tools (https://www.benchling.com), we selected two sgRNAs with high efficiency scores, sg1444 and sg1732, which target the coding sequence region of *ADGRE5* but not the homologous *ADGRE1-4* (Table S2). Besides, these two sgRNAs cover all 4 identified transcripts of *ADGRE5* (Figure S3A). To compare the

Please cite this article in press as: Shang et al., CD97-directed CAR-T cells with enhanced persistence eradicate acute myeloid leukemia in diverse xenograft models, Cell Reports Medicine (2025), https://doi.org/10.1016/j.xcrm.2025.102148

CellPress
OPEN ACCESS

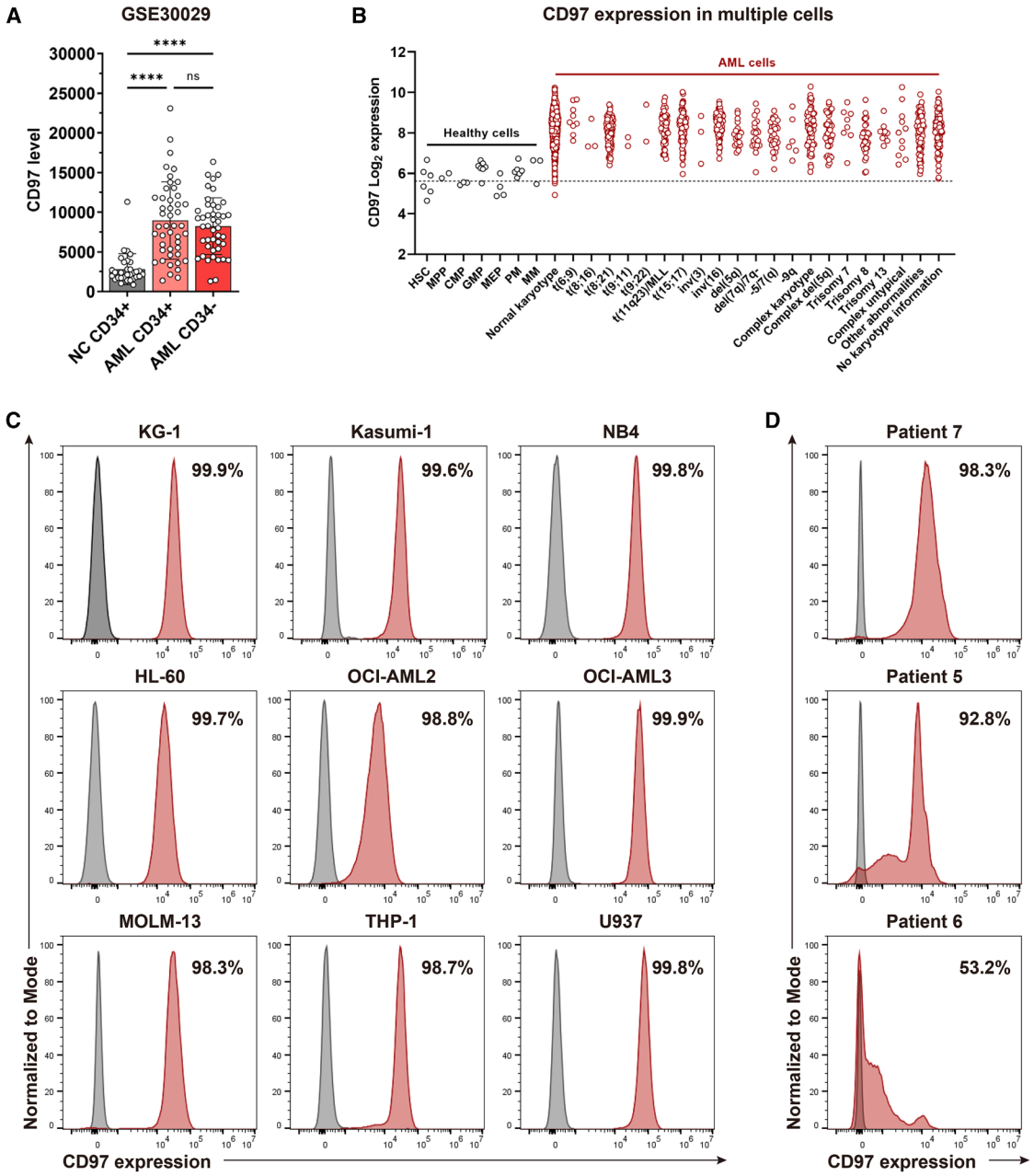

Figure 1. CD97 expression in AML patients and cell lines

(A) CD97 expression in normal CD34$^+$ bone marrow cells ($n = 31$, negative control, NC) and AML bone marrow cells ($n = 46$ or 44) using data from GEO: GSE30029.

(B) CD97 expression level in healthy cells and different karyotypes of AML cells using data from BloodSpot (n = 1,800). HSC, hematopoietic stem cell; MPP, multipotential progenitor; CMP, common myeloid progenitor; GMP, granulocyte monocyte progenitor; MEP, megakaryocyte-erythroid progenitor; PM, promyelocyte; MM, metamyelocyte.

(C and D) Flow cytometry analysis of CD97 expression on (C) AML cell lines and (D) primary patient cells. Histograms show staining with anti-CD97 monoclonal antibody (red) and the isotype control antibody (gray). Inset numbers indicate the CD97 positive percentage.

*$p < 0.05$; **$p < 0.01$; ***$p < 0.001$; ****$p < 0.0001$; ns, not significant.

knockout efficiency of two sgRNAs, we delivered the PX330[45] plasmid containing Cas9 gene and sgRNA into primary T cells by electroporation. The knockout efficiency of sg1444 (29.0%) was much higher than that of sg1732 (5.6%) (Figures S3B and S3C). Consequently, we chose sg1444 for further validation. To further enhance the knockout efficiency, we purified Cas9 protein and synthesized sg1444 to form a ribonucleoprotein (RNP) complex.[46] Indeed, the efficiency of CD97 knockout by sg1444 could reach 67.2% (Figures S3D and S3E). Therefore, we used sg1444 and Cas9 RNP for the subsequent experiments to knock out CD97.

CellPress
OPEN ACCESS

Cell Reports Medicine
Article

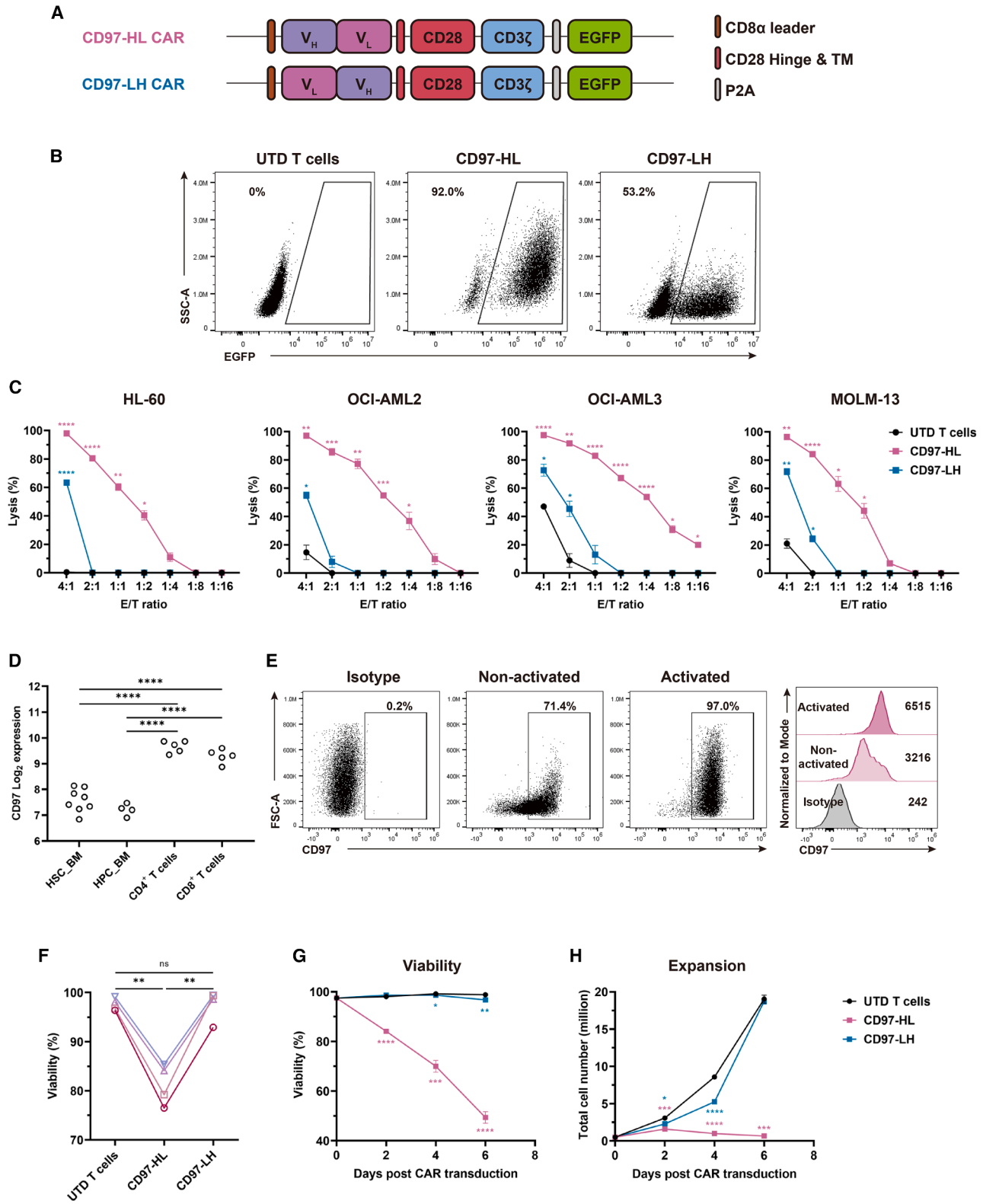

Figure 2. CD97 CAR-T cells recognize and eliminate AML cells *in vitro* but cause fratricide

(A) Schematic of two CD97 CAR constructs. HL and LH stand for two different orders of V_H and V_L in scFv. TM, transmembrane domain; P2A, Porcine teschovirus 2A sequence.

(legend continued on next page)

Please cite this article in press as: Shang et al., CD97-directed CAR-T cells with enhanced persistence eradicate acute myeloid leukemia in diverse xenograft models, Cell Reports Medicine (2025), https://doi.org/10.1016/j.xcrm.2025.102148

A previous study has illustrated that integrating CD19 CAR to the T cell receptor α constant (*TRAC*) locus not only reduced tonic signaling and delayed differentiation but also enhanced anti-tumor potency in an acute lymphoblastic leukemia model compared to CAR-T cells produced by retroviral transduction.[47] Our prior studies have also proved that this strategy is beneficial to CAR-T cells targeting other antigens, such as CD7[48] and CD38.[49] Therefore, we adopted a similar strategy of inserting CD97 CAR to the *TRAC* locus and knocking out *ADGRE5* at the same time, generating *CD97*^{KO}-9728z CAR-T cells (Figure 3A). 7 days after CD97 knockout and CAR transduction, flow cytometry results showed that all CAR-T cells were CD97 negative and enriched to a high CAR-positive percentage (Figure 3B). *CD97*^{KO}-9728z CAR-T cells exhibited potent cytotoxicity against four different AML cell lines (Figure 3C), along with the ability to secrete cytokines and proliferate in an antigen-dependent manner (Figures S4A and S4B). Moreover, *CD97*^{KO}-9728z CAR-T cells had similar viability to untransduced T cells 6 days after CAR transduction (Figure S4C) and showed a 14.55-fold expansion (Figure S4D), suggesting that CD97 knockout could effectively alleviate fratricide.

To evaluate the anti-leukemic activity of *CD97*^{KO}-9728z CAR-T cells *in vivo*, we established a murine xenograft model in which M-NSG mice received tail vein injection of HL-60 cells that were modified to express firefly luciferase (FFLuc). 4 days later, mice received a single dose of 5×10^6 *CD97*^{KO}-9728z CAR-T cells or untransduced T cells (Figure 3D). We found that *CD97*^{KO}-9728z CAR-T cells significantly impeded AML progression and extended survival compared to the untransduced T cells (Figures 3D–3F), which was consistent with the results found using another T cell donor (Figures S4E–S4G). Overall, these data implied that our *CD97*^{KO}-9728z CAR-T strategy combining the insertion of CD97 CAR to *TRAC* locus and deletion of *ADGRE5* mitigated the fratricide and delayed AML progression.

CD97^{KO}-9728z CAR-T cells eliminated primary AML cells while tolerating HSPCs

Next, we evaluated whether our *CD97*^{KO}-9728z CAR-T cells could effectively kill the primary AML cells from patients. We co-cultured CAR-T cells or untransduced T cells with primary AML cells and then quantified the absolute cell number of residual AML cells by flow cytometry (Figure S5A). Our results showed that *CD97*^{KO}-9728z CAR-T cells could specifically eliminate different AML cells from 7 patients (Figure 4A). Though we observed a positive correlation between CD97 expression level in AML specimens and cytotoxicity of CAR-T cells, the difference was not statistically significant at the 1:1 or 2:1 ratio due to the limited sample size (Figure S5B).

On-target, off-tumor toxicity is a major safety concern in CAR-T therapy. To assess the potential hematopoietic toxicity of CD97-targeting CAR-T cells, we co-cultured normal HSPCs with *CD97*^{KO}-9728z CAR-T cells. HSPCs were isolated from umbilical cord blood using CD34-specific microbeads, followed by co-culture with CAR-T cells or untransduced T cells, and subsequently subjected to a colony-forming unit (CFU) assay. Although both $CD34^+CD38^-$ HSCs and $CD34^+CD38^+$ hemopoietic progenitor cells (HPCs) were CD97 positive in two donors, the expression level in HSPCs was much lower than that in AML cell line or activated T cells (Figure 4B). Further, the CFU assay revealed that our CD97-targeting CAR-T cells did not impact HSPCs' multi-lineage differentiation potential compared to control groups (Figure 4C). The direct cytotoxicity assay further indicated a minimal cytotoxic effect on HSCs in comparison to tumor cells (Figure 4D). For BM-derived HSPCs, we tested $CD34^+$ cells obtained from peripheral blood (PB) of a healthy donor treated with mobilizing agents. These cells also expressed CD97 molecule (Figure S5C) and maintained functionality in the CFU assay after co-culturing with CAR-T cells (Figure S5D). However, an increased sensitivity to CAR-T cell-mediated lysis was observed in BM-derived $CD34^+$ cells compared to $CD34^+$ cells sourced from umbilical cord blood (Figures 4D and S5E). Taken together, these data showed that *CD97*^{KO}-9728z CAR-T cells could effectively eliminate various primary AML cells while exerting tolerable toxicity to hematopoiesis, indicating CD97 as a suitable target for AML treatment.

CD97^{KO}-9728z-1XX CAR-T cells displayed superior anti-tumor activity

CD97^{KO}-9728z CAR-T cells exhibited certain anti-tumor effects but were unable to control tumor growth for an extended period even with two injections of CAR-T cells (Figure S6). Additionally, the rapid relapse was not due to the loss of CD97 expression on the tumor cells (Figures S4H and S4I). Therefore, we decided to optimize the co-stimulatory or activation domain of the CAR for better anti-tumor functions. Cytosolic domains of CD28 and 4-1BB are two commonly used co-stimulatory domains in CAR design.[50] Recently, it has been demonstrated that inactivating of the last two ITAMs in CD3ζ of CD28-based CAR could enhance anti-tumor effect of CAR-T cells in both hematologic[51] and solid tumors.[52,53] Hence, we generated *CD97*^{KO}-97BBz and *CD97*^{KO}-9728z-1XX CAR (Figure 5A) to compare with *CD97*^{KO}-9728z CAR.

(B) Representative CD97 CAR expression (EGFP) after transduction of T cells compared to the untransduced (UTD) T cells.
(C) Representative cytotoxicity of indicated CAR-T cells against FFLuc-expressing AML cell lines (HL-60, OCI-AML2, OCI-AML3, and MOLM-13) via co-culturing for 18 h from one of at least 3 independent experiments and donors. Assays were performed in triplicate, and data represent the mean ± SEM. Statistical analysis was conducted between CD97-HL and UTD T cells or CD97-LH and UTD T cells.
(D) CD97 expression on $CD4^+$ and $CD8^+$ T cells compared to normal HSCs and HPCs (hematopoietic progenitor cells) using data from BloodSpot.
(E) Representative CD97 expression levels on non-activated and activated T cells. Isotype antibody was used as a negative control. Inset numbers indicate the CD97-positive percentage or mean fluorescence intensity (MFI).
(F) Viability of UTD T cells, CD97-HL, and CD97-LH CAR-T cells on 2 days after CAR transduction for 4 different donors.
(G) Representative viability changes during *in vitro* expansion from one of at least 3 independent experiments and donors.
(H) Representative expansion results from one of at least 3 independent experiments and donors. Statistical analysis was conducted between CD97-HL and UTD T cells or CD97-LH and UTD T cells.
*$p < 0.05$; **$p < 0.01$; ***$p < 0.001$; ****$p < 0.0001$; ns, not significant.

Please cite this article in press as: Shang et al., CD97-directed CAR-T cells with enhanced persistence eradicate acute myeloid leukemia in diverse xenograft models, Cell Reports Medicine (2025), https://doi.org/10.1016/j.xcrm.2025.102148

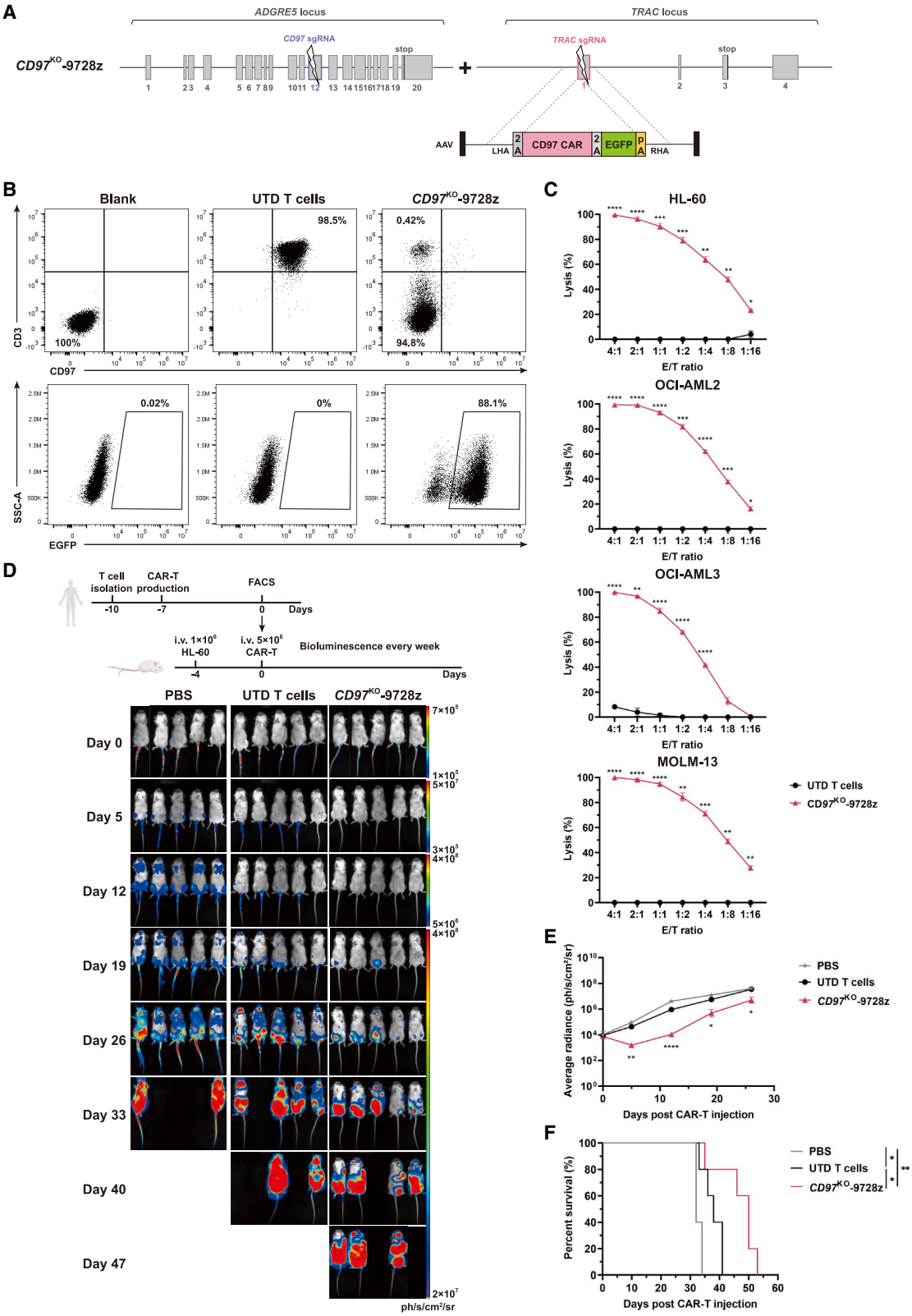

(legend on next page)

Please cite this article in press as: Shang et al., CD97-directed CAR-T cells with enhanced persistence eradicate acute myeloid leukemia in diverse xenograft models, Cell Reports Medicine (2025), https://doi.org/10.1016/j.xcrm.2025.102148

All three CARs had a similar expression level (Figure 5B). Cytotoxicity assay revealed that *CD97*^{KO}-97BBz CAR induced comparable tumor cell lysis to that of *CD97*^{KO}-9728z CAR, while *CD97*^{KO}-9728z-1XX CAR-T cells showed slightly lower cytotoxicity at low E/T ratios against MOLM-13 (Figures 5C and S7A). Meanwhile, *CD97*^{KO}-9728z-1XX CAR-T cells produced the lowest effector cytokines (Figure S7B), consistent with the cytotoxicity results. In the absence of antigen stimulation, all three CAR-T cells showed minimal proliferation, while *CD97*^{KO}-9728z CAR-T cells exhibited greater proliferation than the others after antigen stimulation (Figures S7C–S7E). However, in long-term proliferation assessment with weekly stimulation, *CD97*^{KO}-9728z CAR-T cells lost expansion ability after the second round of stimulation. In contrast, *CD97*^{KO}-9728z-1XX CAR-T cells outperformed the others, achieving more than a 137-fold expansion after two rounds of stimulation (Figure 5D). In experiments involving various T cell donors and tumor models, *CD97*^{KO}-9728z-1XX CAR-T cells consistently displayed superior long-term proliferative capacity (Figure S7F). Furthermore, *CD97*^{KO}-9728z-1XX CAR-T cells demonstrated the lowest expression levels of PD-1 and LAG-3 after stimulation with different tumor cells (Figures S7G and S7H). Notably, *CD97*^{KO}-9728z-1XX CAR-T cells also mitigated cytotoxic effects on HSPCs derived from BM (Figure S5E). However, additional donors are needed to further validate this phenomenon.

In the HL-60 xenograft mouse model, despite all three CAR-T cells exhibiting similar effects in the first two weeks, *CD97*^{KO}-9728z and *CD97*^{KO}-97BBz CAR-T cells eventually lost control of tumor progression (Figures 5E–5G), consistent with the *in vitro* long-term proliferation results (Figures 5D and S7F). In stark contrast, *CD97*^{KO}-9728z-1XX CAR-T cells could achieve complete tumor control (Figures 5E–5G). Meanwhile, in a separate survival study, *CD97*^{KO}-9728z-1XX CAR-T cells significantly extended median survival to 87 days, in contrast to 47 days observed for the other two CAR-T therapies (Figure S8).

To comprehensively evaluate the anti-tumor efficacy of *CD97*^{KO}-9728z-1XX CAR-T cells, we challenged these CAR-T cells in two additional AML xenograft mouse models. In contrast to the M2 subtype HL-60 cells, OCI-AML2 cells exhibited lower level of CD97 expression (Figure S7I) and were classified as M4 subtype.[54] Consistent with the findings in the HL-60 model, *CD97*^{KO}-9728z-1XX CAR-T cells significantly extended median survival to 89 days, compared to 47 days and 54 days for the other two CAR-T cells therapies (Figure S9). In the case of MOLM-13 cells, which are characterized by higher CD97 expression (Figure S7I) and classified as M5 subtype,[54] both *CD97*^{KO}-9728z and *CD97*^{KO}-97BBz CAR-T cells failed to inhibit tumor growth. Conversely, *CD97*^{KO}-9728z-1XX CAR-T cells completely eradicated tumor cells, resulting in sustained complete responses in all five mice (Figures S10A–S10C). Upon tumor rechallenge at day 84, even though they ultimately could not prevent tumor progression, *CD97*^{KO}-9728z-1XX CAR-T cells exhibited some persistence compared to the control group (Figure S10D).

In conclusion, these data indicated that *CD97*^{KO}-9728z-1XX CAR-T cells displayed markedly enhanced persistence and superior anti-AML activity in multiple preclinical mouse models.

CD97^{KO}-9728z-1XX CAR-T cells displayed distinct immunophenotypes and transcriptional signatures

To study why *CD97*^{KO}-9728z-1XX CAR-T cells exhibited superior therapeutic efficacy, we sacrificed mice at day 41 (Figure 5E) in the HL-60 model to analyze the CAR-T cells from blood, spleen, and BM (Figure S16). Only a minimal quantity of tumor cells could be detected in the BM of mice treated with *CD97*^{KO}-9728z-1XX CAR-T cells (Figure 6A). Simultaneously, a substantial number of CAR-T cells were observed in the blood and spleen (Figure S11A). In the BM, the *CD97*^{KO}-9728z-1XX CAR group displayed a significantly higher ratio of CAR-T cell number to tumor cell number (Figure 6B), consistent with the observation of complete remission. Furthermore, the distribution of CD4 and CD8 in *CD97*^{KO}-9728z-1XX CAR-T cells differed significantly from other groups. In either the BM (Figures 6C and 6D) or the spleen (Figures S11B and S11C), *CD97*^{KO}-9728z-1XX CAR-T cells were predominantly composed of CD4-positive cells, while the other two CAR-T cells had a higher proportion of CD8-positive cells.

Immunophenotypic analysis revealed that BM-derived *CD97*^{KO}-9728z-1XX CAR-T cells exhibited a higher proportion of CD45RA^{-}CD62L^{+} central memory and CD45RA^{-}CD62L^{-} effector memory phenotype, accompanied by a lower frequency of CD45RA^{+}CD62L^{-} effector phenotype (Figures 6E and 6F). However, the memory phenotype in CD4^{+} CAR-T cells is different from that in CD8^{+} CAR-T cells derived from BM (Figures S11F–S11I). This memory phenotype pattern was similarly observed in *CD97*^{KO}-9728z-1XX CAR-T cells from the spleen (Figures S11D and S11E). Regarding exhaustion, TIM-3 and LAG-3, but not PD-1, were significantly lower in *CD97*^{KO}-9728z-1XX CAR-T cells

Figure 3. *CD97*^{KO}-9728z CAR-T cells show anti-leukemic activity in AML cell lines both *in vitro* and *in vivo*

(A) Schematic of CRISPR-Cas9-targeted *TRAC* and *ADGRE5* genes knockout and 9728z CAR sequence integration. LHA and RHA, left and right homology arm; 2A, the Porcine teschovirus 2A sequence (dark gray) or Thosea asigna virus 2A sequence (light gray); pA, bovine growth hormone polyA sequence. The rectangles represent the exons of each gene.

(B) Representative CD3, CD97 (top), and CAR (bottom) expression (EGFP) 7 days after *TRAC* and *ADGRE5* genes knockout and CAR sequence integration. Blank means unstained cells as negative control.

(C) Representative cytotoxicity of indicated CAR-T cells against FFLuc-expressing AML cell lines (HL-60, OCI-AML2, OCI-AML3, and MOLM-13) via co-culturing for 18 h from one of at least 3 independent experiments and donors. Assays were performed in triplicate, and data represent the mean ± SEM.

(D) Top: schematic of HL-60 xenograft model following CAR-T therapy. 5×10^6 CAR-T cells were injected 4 days after engraftment of 1×10^6 FFLuc-expressing HL-60 cells. Bottom: representative bioluminescence imaging (BLI) results of tumor burden at indicated days are shown ($n = 5$ for each group).

(E) Kinetics of tumor progression (average radiance) evaluated by BLI. Data are shown as mean ± SEM in log scale. Statistical analysis was conducted between untransduced (UTD) T cells and *CD97*^{KO}-9728z groups.

(F) Kaplan-Meier survival curve of mice treated with PBS, UTD T cells, or *CD97*^{KO}-9728z CAR-T cells.

$^{*}p < 0.05$; $^{**}p < 0.01$; $^{***}p < 0.001$; $^{****}p < 0.0001$; ns, not significant.

Please cite this article in press as: Shang et al., CD97-directed CAR-T cells with enhanced persistence eradicate acute myeloid leukemia in diverse xenograft models, Cell Reports Medicine (2025), https://doi.org/10.1016/j.xcrm.2025.102148

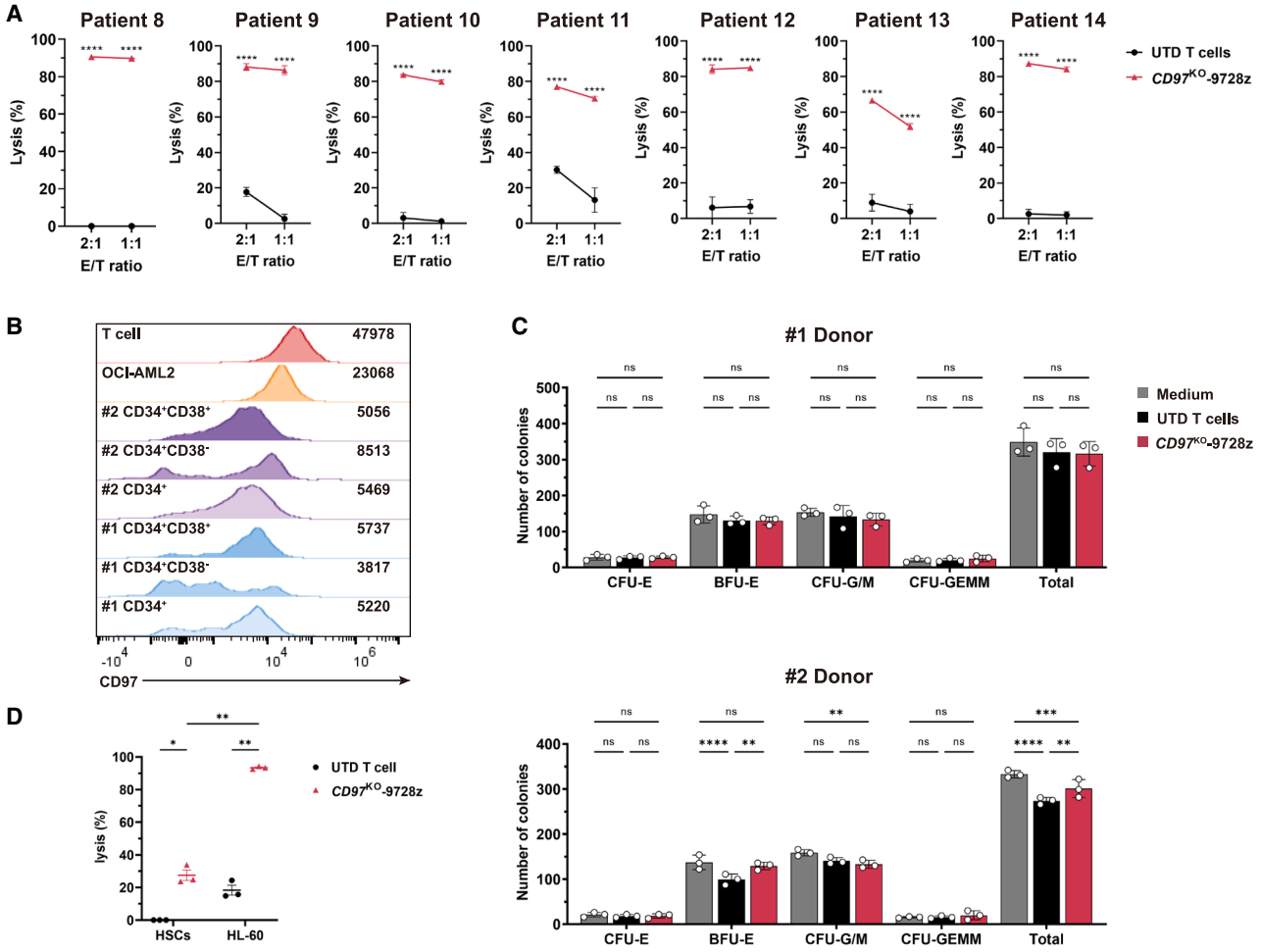

Figure 4. *CD97*^{KO}-9728z CAR-T cells eliminate primary AML specimens while tolerating normal HSPCs

(A) Cytotoxicity of CAR-T cells against primary AML specimens from 7 patients. Assays were performed in triplicate, and data represent the mean ± SEM. UTD, untransduced.

(B) Flow cytometry analysis of CD97 expression on CD34$^+$ HSPCs, CD34$^+$CD38$^-$ HSCs, and CD34$^+$CD38$^+$ HPCs from cord blood of 2 donors. OCI-AML2 cells and activated T cells are used for positive control. Inset numbers indicate the MFI.

(C) CFU assay was performed with residual live HSPCs from 2 donors after 4 h of co-culture with *CD97*^{KO}-9728z CAR-T cells or UTD T cells or medium at an E/T ratio of 1:1 in triplicate. Data show the absolute number of indicated colonies (mean ± SEM). CFU-E, colony-forming unit erythroid; BFU-E, burst-forming unit erythroid; CFU-G/M, colony-forming unit granulocyte/macrophage; CFU-GEMM, colony-forming unit granulocyte, erythrocyte, monocyte, megakaryocyte.

(D) Cytotoxicity of CAR-T cells against HSCs from cord blood. Fresh isolated CD34$^+$CD38$^-$Lin$^-$ HSCs or HL-60 cells were co-cultured with UTD T cells or CAR-T cells or medium at an E/T ratio of 1:1 for 24 h. Assay was performed in triplicate, and data represent the mean ± SEM.

*p < 0.05; **p < 0.01; ***p < 0.001; ****p < 0.0001; ns, not significant.

compared to the other two variants (Figure S12A). *CD97*^{KO}-9728z-1XX CAR-T cells exhibited substantially lower TIM-3$^+$LAG-3$^+$, PD-1-$^+$TIM-3$^+$, or PD-1$^+$LAG-3$^+$ cells than the other two (Figures 6G, 6H, and S12C–S12F). A similar pattern of exhaustion was observed in CAR-T cells derived from the spleen (Figures S12B, S12G, and S12H). These findings indicated that *CD97*^{KO}-9728z-1XX CAR-T cells possessed a less exhausted profile, suggesting a more sustained functional capacity than the alternative CAR-T cell types.

To further characterize their distinct functional and immunophenotypic patterns, we compared the transcriptional profiles of *CD97*^{KO}-9728z-1XX and *CD97*^{KO}-9728z CAR-T cells after three rounds of repeated stimulation with tumor cells *in vitro* (Figure S13A). Principal-component analysis revealed clustering of samples was based on CAR type (Figure S13B). Differential gene analysis indicated that the majority of differentially expressed genes were associated with T cell effector functions, differentiation, and, notably, exhaustion (Figure S13C). As expected, *CD97*^{KO}-9728z CAR-T cells displayed a more pronounced exhaustion profile, characterized by the upregulation of exhaustion-associated markers such as *PDCD1* and *LAG-3*, along with the elevated expression of transcription factors associated with T cell dysfunction, such as *NR4A1-3*, *TBX21*, *BATF*, and *IRF4* (Figure 6I). In alignment with *in vitro* results, genes

Please cite this article in press as: Shang et al., CD97-directed CAR-T cells with enhanced persistence eradicate acute myeloid leukemia in diverse xenograft models, Cell Reports Medicine (2025), https://doi.org/10.1016/j.xcrm.2025.102148

CellPress
OPEN ACCESS

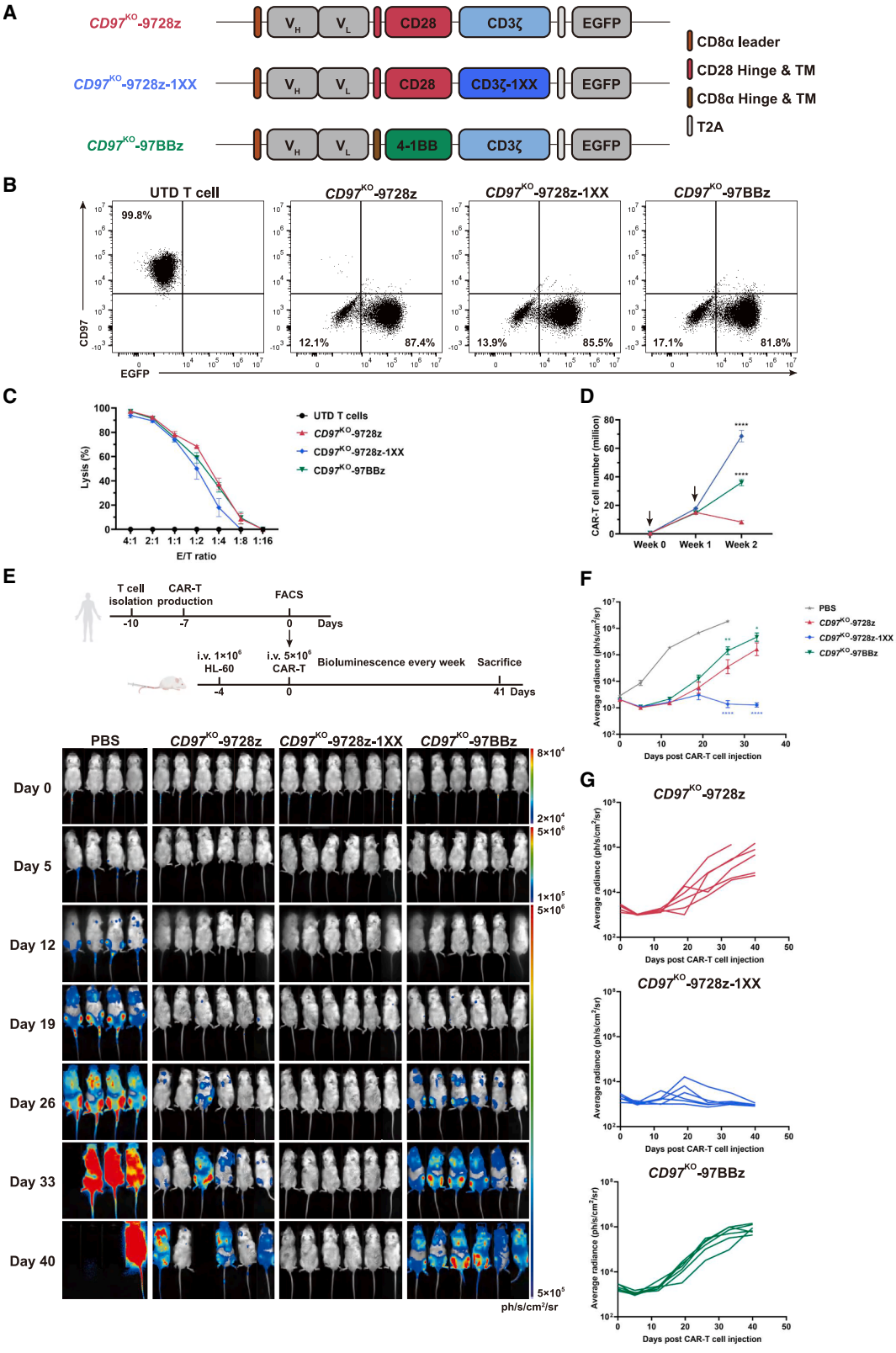

(legend on next page)

up-regulated in *CD97*^{KO}-9728z-1XX CAR-T cells were associated with naive, memory, and effector phenotypes, establishing persistent anti-tumor capability (Figure 6I). Given that CAR uses CD3ζ for downstream signal transduction, the T cell receptor signaling intensity in CAR-T cells can serve as an indicator of CAR signal strength. Gene set enrichment analysis (GSEA) further demonstrated that *CD97*^{KO}-9728z-1XX CAR-T cells exhibited stronger CAR signaling and cytotoxicity, as well as a greater potential for differentiation toward Th1, Th2, or Th17 cells (Figures S13E–S13H). Gene ontology analysis suggested that inflammation- and chemokine-related pathways were down-regulated in *CD97*^{KO}-9728z-1XX CAR-T cells (Figures S13D, S13I, and S13J), which is consistent with lineage differentiation of *CD97*^{KO}-9728z-1XX CAR-T cells and concordant with previous CD3ζ mutation study.[51] Together, we concur with the notion that this finely tuned CAR signal intensity could induce a deceleration of T cell differentiation processes, ultimately leading to more persistent anti-tumor activity.

CD97^{KO}-9728z-1XX CAR-T cells suppressed AML progression and eliminated leukemia stem and progenitor cells in PDX models

We subsequently assessed the therapeutic efficacy of *CD97*^{KO}-9728z-1XX CAR-T cells against heterogeneous primary AML specimens with differing intensity of CD97 expression, different FAB subtypes, and distinct mutational profiles using PDX models. PDX #1 established from engraftment of AML-1, characterized by high percentage expression of the CD97 (Figure S15A) and FAB-M1 subtype (Table S1), was successfully engrafted in the immunodeficient NSG-S mice 7 days post-tail vein injection (Figure S14A). The mice then received a single dose of 5×10^6 *CD97*^{KO}-9728z-1XX CAR-T cells and were observed for tumor progression afterward (Figures 7A and S14B). Our observations indicated that the CAR-T cells effectively suppressed AML progression, resulting in the complete elimination of primary AML cells in both PB (Figure 7B) and BM (Figures 7C and 7D) tissues. In contrast to a typical pallor morphology seen in the femurs and tibias of control mice filled with high leukemia burden, the CAR-T-treated group exhibited a deep red marrow morphology (Figure 7E), suggesting successful restoration of normal hematopoiesis. Furthermore, tSNE analysis of multicolor flow cytometry results revealed the presence of CD34$^+$ CD117$^+$ leukemia stem and progenitor cells (LSPCs) within the BM of control mice, which were completely eradicated in mice that received CAR-T therapy (Figures 7F–7H and S14C).

To functionally validate the efficacy of CAR-T cells in eradicating LSCs, we utilized a secondary transplantation model to measure the activity of LSCs from primary engrafts (Figure 7A). The persistence of AML LSCs was evident in the control group, as AML recurred and progressed upon secondary transplantation (Figures 7I and 7J). Moreover, the morphology of the femurs and tibias from control mice exhibited a high leukemia burden (Figures S14D and S14E). In contrast, no AML cells were detectable in the PB or BM of mice following secondary engraftment with cells from the CAR-T treatment group (Figures 7I, 7J, and S14D–S14E). Similar results were observed in another PDX model engrafted with AML2 with a differing FAB-M5b subtype and mutational profile (Table S1), expressing CD97 at a different intensity (Figure S15). Collectively, these data robustly illustrated the potent efficacy of *CD97*^{KO}-9728z-1XX CAR-T cells in eliminating both bulk and LSPCs in primary AML cells, despite their phenotypic and genetic heterogeneity.

DISCUSSION

Over the past decade, CAR-T therapy has demonstrated remarkable success in treating hematopoietic malignancies, particularly in B cell malignancies and multiple myeloma. However, one major challenge of CAR-T therapy in AML is a suitable target. Many targets are not exclusive to AML blasts and are also expressed on normal HSPCs. Clinical trials showed that CAR-T cells targeting CD33[18] or CD123[19] are effective for AML. Nevertheless, these antigens are present on normal HSPCs,[30] raising concerns about hematopoietic toxicity following adoptive cell therapy. Consequently, HSC transplantation has become necessary to reconstitute normal hematopoiesis.[25,26,28–30] In addition to clinical insights, large-scale omics analyses make valuable contributions to overcoming these obstacles. Recent reports have identified potential targets for CAR-T therapy in AML, including ADGRE2, CCR1, CD70, and LILRB2 in one study[55] and CSF1R and CD86 in another study,[56] demonstrating their effectiveness in eliminating AML blasts and safety in sparing HSCs. The expanding tool library for CAR-T therapy in AML indicates a promising trend toward greater diversity in target selection in the future.

In this context, we present CD97 as a feasible target for CAR-T therapy in AML. Previous studies have shown that CD97 is not

Figure 5. *CD97*^{KO}-9728z-1XX CAR-T cells exhibit persistence and effectively control AML in a xenograft model

(A) Schematic of three different CAR designs. TM, transmembrane domain; T2A, Thosea asigna virus 2A sequence.

(B) Representative CD97 and CAR expression (EGFP) on 7 days after *TRAC* and *ADGRE5* genes knockout and CAR sequence integration. UTD, untransduced.

(C) Representative cytotoxicity of indicated CAR-T cells against FFLuc-expressing HL-60 cells via co-culturing for 18 h from one of at least 3 independent experiments and donors. Assay was performed in triplicate, and data represent the mean ± SEM.

(D) Representative cumulative cell numbers of indicated CAR-T cells upon weekly stimulation with HL-60 cells. Data represent the mean ± SEM of triplicates. Statistical analysis was performed comparing *CD97*^{KO}-9728z-1XX or *CD97*^{KO}-97BBz to *CD97*^{KO}-9728z. Arrows mean we stimulated CAR-T cells with HL-60 cells at the indicated time.

(E) Top: schematic of HL-60 xenograft model following CAR-T therapy. 5×10^6 CAR-T cells were injected 4 days after engraftment of 1×10^6 FFLuc-expressing HL-60 cells. Bottom: representative BLI results of tumor burden at indicated days are shown (n = 4 or 6 for each group).

(F) Kinetics of tumor progression (average radiance) evaluated by BLI. Data are shown as mean ± SEM in log scale. Statistical analysis was shown comparing *CD97*^{KO}-9728z-1XX or *CD97*^{KO}-97BBz to *CD97*^{KO}-9728z.

(G) Tumor burden of mice in each group is shown.

$^*p < 0.05$; $^{**}p < 0.01$; $^{***}p < 0.001$; $^{****}p < 0.0001$; ns, not significant.

Please cite this article in press as: Shang et al., CD97-directed CAR-T cells with enhanced persistence eradicate acute myeloid leukemia in diverse xenograft models, Cell Reports Medicine (2025), https://doi.org/10.1016/j.xcrm.2025.102148

CellPress
OPEN ACCESS

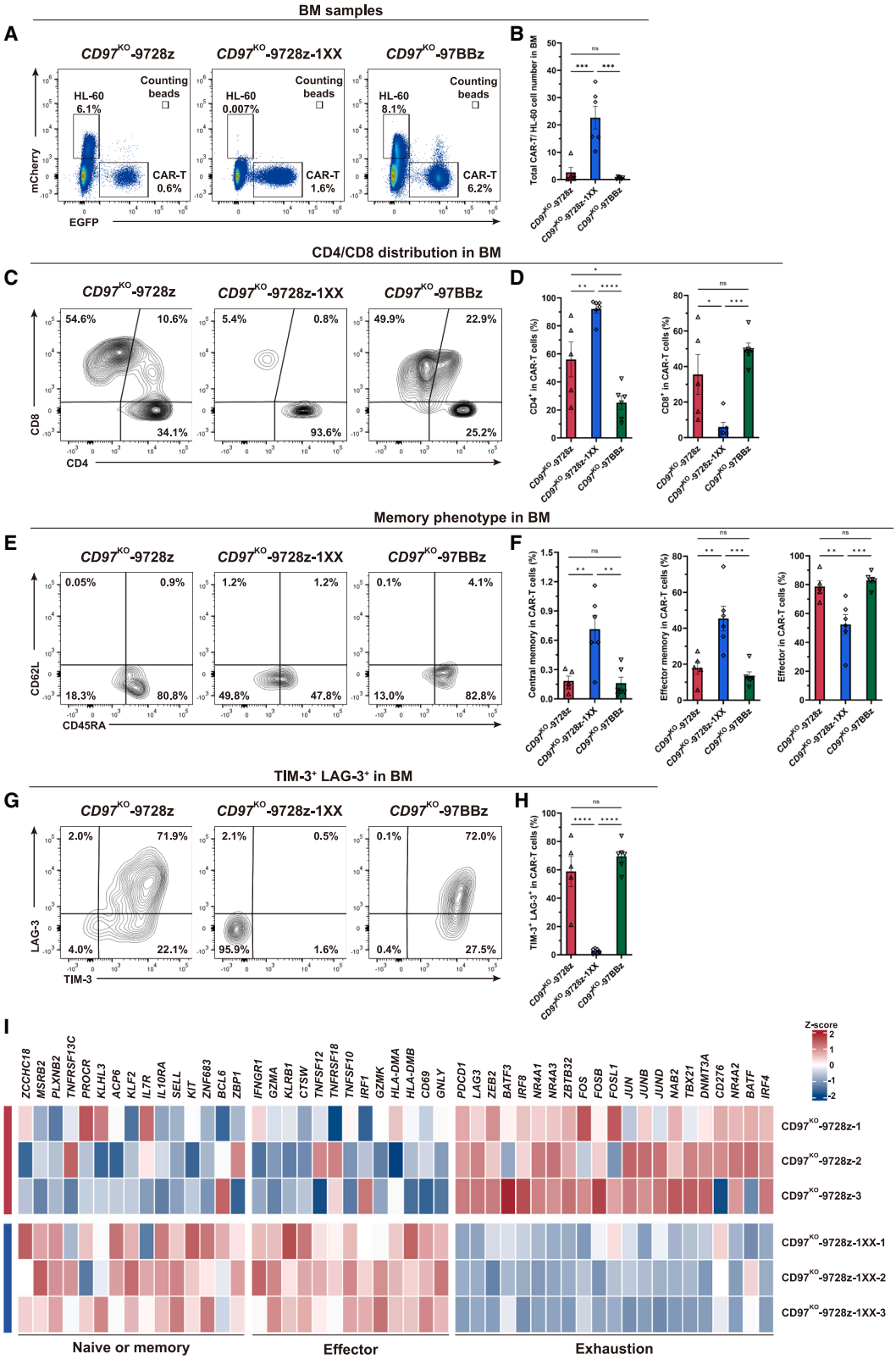

(legend on next page)

Please cite this article in press as: Shang et al., CD97-directed CAR-T cells with enhanced persistence eradicate acute myeloid leukemia in diverse xenograft models, Cell Reports Medicine (2025), https://doi.org/10.1016/j.xcrm.2025.102148

only up-regulated in AML patients and LSCs but also important for the proliferation and survival of AML blasts and LSCs.[37–41] As an aGPCR, CD97 activation requires autoproteolysis at a conserved G protein-coupled receptor proteolysis site upon ligand binding or mechanical force.[57,58] The structure of CD97's active conformation was only revealed recently.[59,60] Currently, except for a CD97-targeting antibody-drug conjugate for glioblastoma,[61] no CD97-related drugs have been reported. Thus, CAR-T cells could be an alternative approach to target CD97-expressing tumor cells, such as AML.

Our data revealed that CD97 was up-regulated in nearly all AML patients compared to normal HSCs, providing a broader scope of coverage than existing targets such as CD33, CD123, and CLL-1 that are currently under investigation in clinical trials. In our collection of 14 AML patients, all the samples exhibited positive CD97 expression. Moreover, our CD97 CAR-T cells effectively eliminated AML cells derived from diverse patient samples. CD97 expression extended to different AML cell lines across varied FAB subtypes, consistent with CD97-targeting CAR-T cell's efficacy in both *in vitro* and *in vivo* models. Importantly, the expression level of CD97 on $CD34^+$ HSPCs derived from cord blood or BM was notably lower than that observed in AML cell lines or activated T cells. Furthermore, CFU assay indicated negligible toxicity to HSPCs. These results collectively demonstrate that CD97 is a suitable target for CAR-T therapy in AML.

Given that CD97 is also expressed on the surface of T cells, CD97 CAR-T cells would encounter fratricide during expansion. To address this issue, we employed a strategy involving the knockout of CD97 encoded gene, *ADGRE5*, and the insertion of CD97 CAR transgene into the *TRAC* locus by CRISPR-Cas9 simultaneously. This approach markedly alleviated fratricide, enabling normal expansion of CAR-T cells.

However, the *in vivo* performance of the original $CD97^{KO}$-9728z CAR-T cells fell short of our expectations. Consequently, we optimized the CAR design by fine-tuning CD3ζ signaling through mutations in the last two ITAMs. The refined $CD97^{KO}$-9728z-1XX CAR-T cells showed outstanding and persistent anti-tumor effects, thoroughly eliminating tumor cells in partial xenograft models. Moreover, they also mitigated cytotoxicity on HSPCs. Immunophenotypic and transcriptional signatures revealed that $CD97^{KO}$-9728z-1XX CAR-T cells exhibited more memory-differentiated profiles and less exhaustion. Previous study showed that CD19-targeting CAR-T cells with the CD28 co-stimulatory domain (1928z) displayed an effector phenotype and 1928z-1XX CAR-T cells exhibited memory phenotype after single stimulation by antigen-presenting cells.[51] However, 9728z CAR-T cells in our study displayed an exhausted phenotype after three repeated stimulations, while 9728z-1XX showed not only a memory phenotype but also an effector phenotype. These results align with our more challenging repeated-stimulation conditions, leading to more activation and stimulation of CAR-T cells. Nevertheless, in both CD19- and CD97-targeting CAR-T models, 1XX CAR-T cells with only one ITAM showed delayed differentiation and persistent anti-tumor activities compared to their wild-type CAR-T cell counterparts, which is consistent with several CAR-T studies targeting other antigens.[51–53] Thus, mutating CD3ζ to 1XX in different CAR-T cells is an effective and generalizable strategy to enhance CAR-T cell functions.

AML arises from and is maintained by LSCs, leading to resistance to standard therapies and frequent relapse.[10–12,62] Targeting LSCs may be crucial for curing AML. However, cell line-derived xenograft (CDX) models cannot effectively investigate LSC functionality due to their homogeneous nature. In contrast, PDX models preserve the original characteristics of the primary tumor, including disease heterogeneity and LSCs, making them powerful tools for cancer research.[63] As anticipated, our $CD97^{KO}$-9728z-1XX CAR-T cells eliminated all AML cells, including immunophenotypically and functionally defined LSPCs, in two different AML PDX models, demonstrating remarkable anti-leukemic activity.

In summary, our study establishes CD97 as a suitable target for CAR-T therapy in treating AML. The engineered CD97 CAR-T cells exhibit potent anti-leukemic activity *in vitro*, in CDX models and PDX models, while displaying tolerable toxicity to HSPCs, suggesting that CD97 CAR-T cell therapy holds significant promise as an effective treatment for AML.

Limitations of the study

In our study, the CD97 knockout efficiency was not optimal, with approximately 30% of T or CAR-T cells still expressing CD97 on their surface. This residual expression may induce moderate fratricide, potentially affecting the therapeutic efficacy *in vivo*. To address this, optimized sgRNAs are needed to improve the knockout efficiency. Additionally, the safety assessment was conducted exclusively *in vitro*. Further *in vivo* investigations using humanized CD97 mice would provide a more comprehensive evaluation of the safety profile of our CD97-targeting CAR-T cells, which is important for clinical translation.

RESOURCE AVAILABILITY

Lead contact

Further information and requests for resources and reagents should be directed to and will be fulfilled by the lead contact, Jie Sun (sunj4@zju.edu.cn).

Figure 6. $CD97^{KO}$-9728z-1XX CAR-T cells display distinct immunophenotypes

Mice were sacrificed at day 41 post-CAR-T cell injection (n = 5 or 6 for each group).

(A) Representative HL-60 and CAR-T cell percentages in bone marrow. Absolute HL-60 and CAR-T cell number were calculated by counting beads.

(B) Statistics for the ratio of total CAR-T cell number/HL-60 cell number in bone marrow.

(C and D) (C) Representative $CD4^+$ and $CD8^+$ distribution in CAR-T cells and (D) statistics in bone marrow.

(E and F) (E) Representative memory phenotype of CAR-T cells in bone marrow determined by CD45RA and CD62L and (F) statistics for central memory ($CD45RA^-CD62L^+$), effector memory ($CD45RA^-CD62L^-$), and effector phenotypes ($CD45RA^+CD62L^-$).

(G and H) (G) Representative exhaustion phenotype of CAR-T cells in bone marrow distinguished by TIM-3 and LAG-3 and (H) statistics. Data are shown as mean ± SEM.

(I) Heatmap for selected genes related to indicated T cell phenotypes, including naive, memory, effector, and exhaustion.

$^*p < 0.05$; $^{**}p < 0.01$; $^{***}p < 0.001$; $^{****}p < 0.0001$; ns, not significant.

Please cite this article in press as: Shang et al., CD97-directed CAR-T cells with enhanced persistence eradicate acute myeloid leukemia in diverse xenograft models, Cell Reports Medicine (2025), https://doi.org/10.1016/j.xcrm.2025.102148

CellPress
OPEN ACCESS

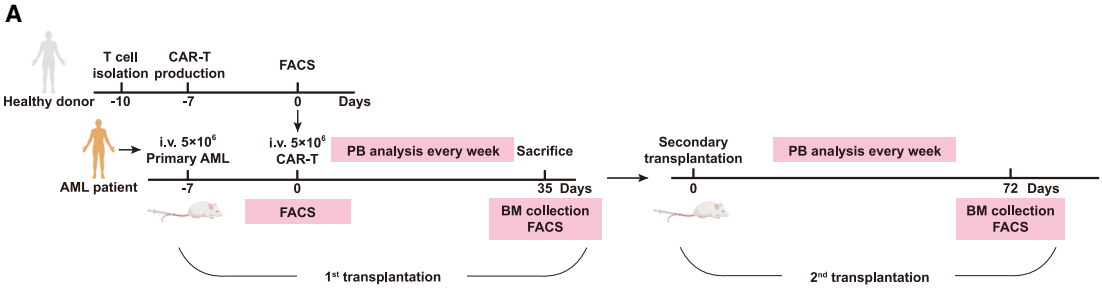

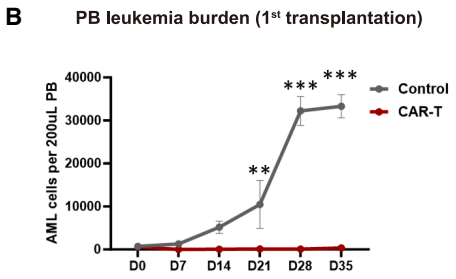

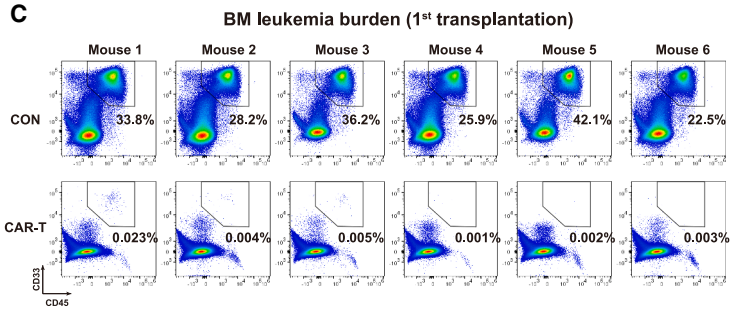

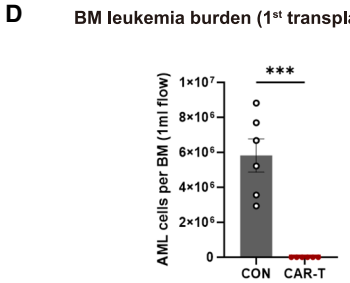

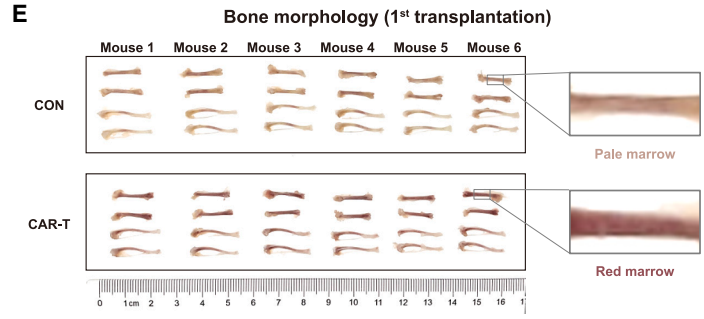

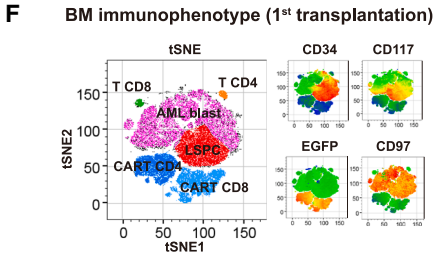

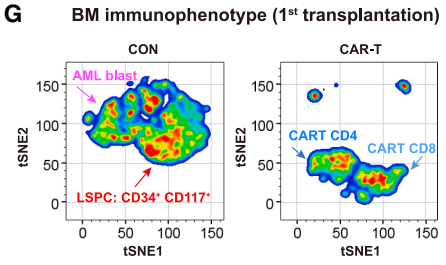

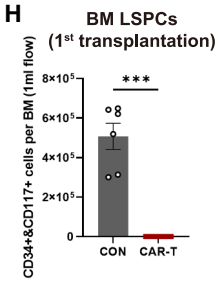

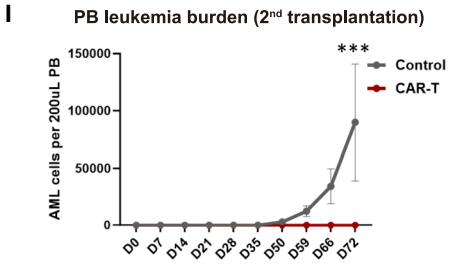

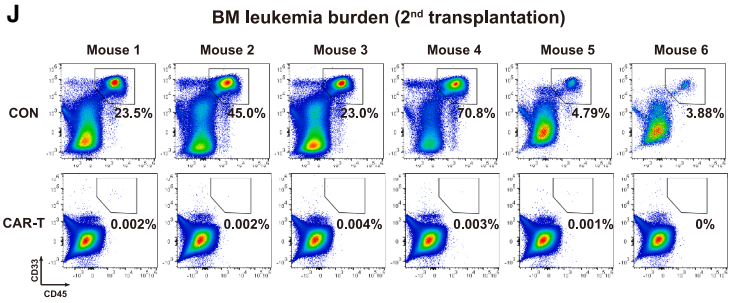

(legend on next page)

Materials availability

Plasmids requests can be directed to the lead contact.

Data and code availability

- RNA sequencing data have been deposited at China National GeneBank (CNGB) databaseCNGB: CNP0007174 and are publicly available as of the date of publication.
- This paper does not report original code.
- Any additional information required to reanalyze the data reported in this paper is available from the lead contact upon request.

ACKNOWLEDGMENTS

This work was supported by the National Key R&D Program of China grants 2021YFA0909900 (J.S., author 22) and 2022YFA1103500 (P.Q.); the National Natural Science Foundation of China grants 82161138028 (J.S., author 22), 82222003 (P.Q.), 92268117 (P.Q.), 82470149 (S.P.), 82270157 (S.P.), 82400207 (J.L.), and 82400179 (L.L.); Zhejiang Provincial Natural Science Foundation grants LR20H160003 (J.S., author 22), Z24H080001 (P.Q.), and LQ24H080008 (L.L.); the Leading Innovative and Entrepreneur Team Introduction Program of Zhejiang grant 2020R01006 (J.S., author 22); the Key R&D Program of Zhejiang grants 2024SSYS0024 (P.Q.) and 2022C03005 (S.P.); the Department of Science and Technology of Zhejiang Province grants 2023R01012 (P.Q.) and 2023R01012 (S.P.); and the Fundamental Research Funds for the Central Universities grant 226-2024-00007 (P.Q.). The authors thank the support of the Zhejiang Provincial Key Laboratory of Immunity and Inflammatory Diseases. The authors also thank Yingying Huang, Jiajia Wang, Chun Guo, and Yueting Xing from the Core Facilities, Zhejiang University School of Medicine, and Zhengyan Wang from Laboratory Animal Center, Zhejiang University, for their technical support.

AUTHOR CONTRIBUTIONS

K.S., D.H., Y.D., J.L., H.H., S.P., P.Q., and Jie Sun (author 22) designed the studies and conceived the experiments; K.S., D.H., J.L., W.B., J.C., J.J., and Y.W. performed the experiments; K.S., D.H., J.L., and Z.Y. analyzed data; J.G., S.Z., and Y. Han. contributed reagents; K.S., D.H., J.L., W.B., Y. Z., L.L., J.G., and S.Z. took care of the mice; Jie Sun (author 18), Y. Hu., and W.Z. provided the patient sample. K.S., C.Z., S.P., P.Q., and Jie Sun (author 22) wrote and revised the manuscript; H.H., S.P., P.Q., and Jie Sun (author 22) supervised the study.

DECLARATION OF INTERESTS

The authors declare no competing interests.

STAR★METHODS

Detailed methods are provided in the online version of this paper and include the following:

SUPPLEMENTAL INFORMATION

Supplemental information can be found online at https://doi.org/10.1016/j.xcrm.2025.102148.

Received: February 15, 2024
Revised: November 11, 2024
Accepted: April 30, 2025
Published: May 26, 2025

REFERENCES

1. Döhner, H., Weisdorf, D.J., and Bloomfield, C.D. (2015). Acute Myeloid Leukemia. N. Engl. J. Med. Overseas. Ed. *373*, 1136–1152. https://doi.org/10.1056/NEJMra1406184.
2. Khwaja, A., Bjorkholm, M., Gale, R.E., Levine, R.L., Jordan, C.T., Ehninger, G., Bloomfield, C.D., Estey, E., Burnett, A., Cornelissen, J.J., et al. (2016). Acute myeloid leukaemia. Nat. Rev. Dis. Primers *2*, 16010. https://doi.org/10.1038/nrdp.2016.10.
3. DiNardo, C.D., Erba, H.P., Freeman, S.D., and Wei, A.H. (2023). Acute myeloid leukaemia. Lancet *401*, 2073–2086. https://doi.org/10.1016/S0140-6736(23)00108-3.
4. Ferrara, F., and Schiffer, C.A. (2013). Acute myeloid leukaemia in adults. Lancet *381*, 484–495. https://doi.org/10.1016/S0140-6736(12)61727-9.

Figure 7. *CD97*^{KO}-9728z-1XX CAR-T cells inhibit AML progression in the PDX model and eliminate LSPCs to prevent relapse

(A) Schematic of the PDX model receiving CAR-T therapy (n = 6 for each group).
(B) Kinetics of tumor progression evaluated by AML cell number from peripheral blood (PB) using flow cytometry. Data are shown as mean ± SEM.
(C and D) (C) Flow cytometry and (D) statistical analysis of tumor burden (CD45$^+$CD33$^+$) in bone marrow of 1st transplantation from control and CAR-T-treated groups. Data are shown as mean ± SEM.
(E) Morphology of bone marrow for each mouse from 1st transplantation.
(F) tSNE analysis of all bone marrow samples from 1st transplantation. T, CAR-T, AML blast, and LSPC subpopulations were defined by expression of EGFP, CD34, CD117, CD97, and others.
(G) tSNE plots of control (CON) group versus CAR-T groups. The analysis shows that the CON group contained AML blasts and CD34$^+$ CD117$^+$ LSPCs while CAR-T group only had CAR-T cells or untransduced T cells.
(H) Statistical analysis of number of LSPCs in control and CAR-T group from 1st transplantation. Data are shown as mean ± SEM.
(I) Kinetics of tumor progression in 2nd transplantation evaluated by AML cell number from peripheral blood (PB) using flow cytometry. Data are shown as mean ± SEM.
(J) Tumor burden of primary AML cells (CD45$^+$ CD33$^+$) in bone marrow from 2nd transplantation.
$^*p < 0.05$; $^{**}p < 0.01$; $^{***}p < 0.001$; $^{****}p < 0.0001$; ns, not significant.

5. Vago, L., and Gojo, I. (2020). Immune escape and immunotherapy of acute myeloid leukemia. J. Clin. Investig. *130*, 1552–1564. https://doi.org/10.1172/JCI129204.

6. Marofi, F., Rahman, H.S., Al-Obaidi, Z.M.J., Jalil, A.T., Abdelbasset, W.K., Suksatan, W., Dorofeev, A.E., Shomali, N., Chartrand, M.S., Pathak, Y., et al. (2021). Novel CAR T therapy is a ray of hope in the treatment of seriously ill AML patients. Stem Cell Res. Ther. *12*, 465. https://doi.org/10.1186/s13287-021-02420-8.

7. Walter, R.B., Othus, M., Burnett, A.K., Löwenberg, B., Kantarjian, H.M., Ossenkoppele, G.J., Hills, R.K., Ravandi, F., Pabst, T., Evans, A., et al. (2015). Resistance prediction in AML: analysis of 4601 patients from MRC/NCRI, HOVON/SAKK, SWOG and MD Anderson Cancer Center. Leukemia *29*, 312–320. https://doi.org/10.1038/leu.2014.242.

8. de Boer, B., Prick, J., Pruis, M.G., Keane, P., Imperato, M.R., Jaques, J., Brouwers-Vos, A.Z., Hogeling, S.M., Woolthuis, C.M., Nijk, M.T., et al. (2018). Prospective Isolation and Characterization of Genetically and Functionally Distinct AML Subclones. Cancer Cell *34*, 674–689.e8. https://doi.org/10.1016/j.ccell.2018.08.014.

9. Zeng, A.G.X., Bansal, S., Jin, L., Mitchell, A., Chen, W.C., Abbas, H.A., Chan-Seng-Yue, M., Voisin, V., van Galen, P., Tierens, A., et al. (2022). A cellular hierarchy framework for understanding heterogeneity and predicting drug response in acute myeloid leukemia. Nat. Med. *28*, 1212–1223. https://doi.org/10.1038/s41591-022-01819-x.

10. Ding, L., Ley, T.J., Larson, D.E., Miller, C.A., Koboldt, D.C., Welch, J.S., Ritchey, J.K., Young, M.A., Lamprecht, T., McLellan, M.D., et al. (2012). Clonal evolution in relapsed acute myeloid leukaemia revealed by whole-genome sequencing. Nature *481*, 506–510. https://doi.org/10.1038/nature10738.

11. Thomas, D., and Majeti, R. (2017). Biology and relevance of human acute myeloid leukemia stem cells. Blood *129*, 1577–1585. https://doi.org/10.1182/blood-2016-10-696054.

12. Pei, S., Pollyea, D.A., Gustafson, A., Stevens, B.M., Minhajuddin, M., Fu, R., Riemondy, K.A., Gillen, A.E., Sheridan, R.M., Kim, J., et al. (2020). Monocytic Subclones Confer Resistance to Venetoclax-Based Therapy in Patients with Acute Myeloid Leukemia. Cancer Discov. *10*, 536–551. https://doi.org/10.1158/2159-8290.CD-19-0710.

13. June, C.H., and Sadelain, M. (2018). Chimeric Antigen Receptor Therapy. N. Engl. J. Med. *379*, 64–73. https://doi.org/10.1056/NEJMra1706169.

14. Baker, D.J., Arany, Z., Baur, J.A., Epstein, J.A., and June, C.H. (2023). CAR T therapy beyond cancer: the evolution of a living drug. Nature *619*, 707–715. https://doi.org/10.1038/s41586-023-06243-w.

15. Park, J.H., Rivière, I., Gonen, M., Wang, X., Sénéchal, B., Curran, K.J., Sauter, C., Wang, Y., Santomasso, B., Mead, E., et al. (2018). Long-Term Follow-up of CD19 CAR Therapy in Acute Lymphoblastic Leukemia. N. Engl. J. Med. Overseas. Ed. *378*, 449–459. https://doi.org/10.1056/NEJMoa1709919.

16. Munshi, N.C., Anderson, L.D., Shah, N., Madduri, D., Berdeja, J., Lonial, S., Raje, N., Lin, Y., Siegel, D., Oriol, A., et al. (2021). Idecabtagene Vicleucel in Relapsed and Refractory Multiple Myeloma. N. Engl. J. Med. *384*, 705–716. https://doi.org/10.1056/NEJMoa2024850.

17. Peinert, S., Prince, H.M., Guru, P.M., Kershaw, M.H., Smyth, M.J., Trapani, J.A., Gambell, P., Harrison, S., Scott, A.M., Smyth, F.E., et al. (2010). Gene-modified T cells as immunotherapy for multiple myeloma and acute myeloid leukemia expressing the Lewis Y antigen. Gene Ther. *17*, 678–686. https://doi.org/10.1038/gt.2010.21.

18. Kenderian, S.S., Ruella, M., Shestova, O., Klichinsky, M., Aikawa, V., Morrissette, J.J.D., Scholler, J., Song, D., Porter, D.L., Carroll, M., et al. (2015). CD33-specific chimeric antigen receptor T cells exhibit potent preclinical activity against human acute myeloid leukemia. Leukemia *29*, 1637–1647. https://doi.org/10.1038/leu.2015.52.

19. Mardiros, A., Dos Santos, C., McDonald, T., Brown, C.E., Wang, X., Budde, L.E., Hoffman, L., Aguilar, B., Chang, W.-C., Bretzlaff, W., et al. (2013). T cells expressing CD123-specific chimeric antigen receptors exhibit specific cytolytic effector functions and antitumor effects against human acute myeloid leukemia. Blood *122*, 3138–3148. https://doi.org/10.1182/blood-2012-12-474056.

20. Casucci, M., Nicolis di Robilant, B., Falcone, L., Camisa, B., Norelli, M., Genovese, P., Gentner, B., Gullotta, F., Ponzoni, M., Bernardi, M., et al. (2013). CD44v6-targeted T cells mediate potent antitumor effects against acute myeloid leukemia and multiple myeloma. Blood *122*, 3461–3472. https://doi.org/10.1182/blood-2013-04-493361.

21. Wang, J., Chen, S., Xiao, W., Li, W., Wang, L., Yang, S., Wang, W., Xu, L., Liao, S., Liu, W., et al. (2018). CAR-T cells targeting CLL-1 as an approach to treat acute myeloid leukemia. J. Hematol. Oncol. *11*, 7. https://doi.org/10.1186/s13045-017-0553-5.

22. Jetani, H., Garcia-Cadenas, I., Nerreter, T., Thomas, S., Rydzek, J., Meijide, J.B., Bonig, H., Herr, W., Sierra, J., Einsele, H., and Hudecek, M. (2018). CAR T-cells targeting FLT3 have potent activity against FLT3−ITD+ AML and act synergistically with the FLT3-inhibitor crenolanib. Leukemia *32*, 1168–1179. https://doi.org/10.1038/s41375-018-0009-0.

23. Sauer, T., Parikh, K., Sharma, S., Omer, B., Sedloev, D., Chen, Q., Angenendt, L., Schliemann, C., Schmitt, M., Müller-Tidow, C., et al. (2021). CD70-specific CAR T cells have potent activity against acute myeloid leukemia without HSC toxicity. Blood *138*, 318–330. https://doi.org/10.1182/blood.2020008221.

24. Jetani, H., Navarro-Bailón, A., Maucher, M., Frenz, S., Verbruggen, C., Yeguas, A., Vidriales, M.B., González, M., Rial Saborido, J., Kraus, S., et al. (2021). Siglec-6 is a novel target for CAR T-cell therapy in acute myeloid leukemia. Blood *138*, 1830–1842. https://doi.org/10.1182/blood.2020009192.

25. Wang, Q.-s., Wang, Y., Lv, H.-y., Han, Q.-w., Fan, H., Guo, B., Wang, L.-l., and Han, W.-d. (2015). Treatment of CD33-directed Chimeric Antigen Receptor-modified T Cells in One Patient With Relapsed and Refractory Acute Myeloid Leukemia. Mol. Ther. *23*, 184–191. https://doi.org/10.1038/mt.2014.164.

26. Budde, L., Song, J.Y., Kim, Y., Blanchard, S., Wagner, J., Stein, A.S., Weng, L., Del Real, M., Hernandez, R., Marcucci, E., et al. (2017). Remissions of Acute Myeloid Leukemia and Blastic Plasmacytoid Dendritic Cell Neoplasm Following Treatment with CD123-Specific CAR T Cells: A First-in-Human Clinical Trial. Blood *130*, 811. https://doi.org/10.1182/blood.V130.Suppl_1.811.811.

27. Jin, X., Zhang, M., Sun, R., Lyu, H., Xiao, X., Zhang, X., Li, F., Xie, D., Xiong, X., Wang, J., et al. (2022). First-in-human phase I study of CLL-1 CAR-T cells in adults with relapsed/refractory acute myeloid leukemia. J. Hematol. Oncol. *15*, 88. https://doi.org/10.1186/s13045-022-01308-1.

28. Tambaro, F.P., Singh, H., Jones, E., Rytting, M., Mahadeo, K.M., Thompson, P., Daver, N., DiNardo, C., Kadia, T., Garcia-Manero, G., et al. (2021). Autologous CD33-CAR-T cells for treatment of relapsed/refractory acute myelogenous leukemia. Leukemia *35*, 3282–3286. https://doi.org/10.1038/s41375-021-01232-2.

29. Naik, S., Madden, R.M., Lipsitt, A., Lockey, T., Bran, J., Rubnitz, J.E., Klco, J., Shulkin, B., Patil, S.L., Schell, S., et al. (2022). Safety and Anti-Leukemic Activity of CD123-CAR T Cells in Pediatric Patients with AML: Preliminary Results from a Phase 1 Trial. Blood *140*, 4584–4585. https://doi.org/10.1182/blood-2022-170201.

30. Ehninger, A., Kramer, M., Röllig, C., Thiede, C., Bornhäuser, M., von Bonin, M., Wermke, M., Feldmann, A., Bachmann, M., Ehninger, G., and Oelschlägel, U. (2014). Distribution and levels of cell surface expression of CD33 and CD123 in acute myeloid leukemia. Blood Cancer J. *4*, e218. https://doi.org/10.1038/bcj.2014.39.

31. Steinert, M., Wobus, M., Boltze, C., Schütz, A., Wahlbuhl, M., Hamann, J., and Aust, G. (2002). Expression and Regulation of CD97 in Colorectal Carcinoma Cell Lines and Tumor Tissues. Am. J. Pathol. *161*, 1657–1667. https://doi.org/10.1016/S0002-9440(10)64443-4.

32. Ward, Y., Lake, R., Martin, P.L., Killian, K., Salerno, P., Wang, T., Meltzer, P., Merino, M., Cheng, S.y., Santoro, M., et al. (2013). CD97 amplifies LPA

receptor signaling and promotes thyroid cancer progression in a mouse model. Oncogene *32*, 2726–2738. https://doi.org/10.1038/onc.2012.301.

33. Yin, Y., Xu, X., Tang, J., Zhang, W., Zhangyuan, G., Ji, J., Deng, L., Lu, S., Zhuo, H., and Sun, B. (2018). CD97 Promotes Tumor Aggressiveness Through the Traditional G Protein–Coupled Receptor–Mediated Signaling in Hepatocellular Carcinoma. Hepatology *68*, 1865–1878. https://doi.org/10.1002/hep.30068.

34. Liu, D., Trojanowicz, B., Radestock, Y., Fu, T., Hammje, K., Chen, L., and Hoang-Vu, C. (2010). Role of CD97 isoforms in gastric carcinoma. Int. J. Oncol. *36*, 1401–1408. https://doi.org/10.3892/ijo_00000625.

35. Safaee, M., Clark, A.J., Oh, M.C., Ivan, M.E., Bloch, O., Kaur, G., Sun, M. Z., Kim, J.M., Oh, T., Berger, M.S., and Parsa, A.T. (2013). Overexpression of CD97 Confers an Invasive Phenotype in Glioblastoma Cells and Is Associated with Decreased Survival of Glioblastoma Patients. PLoS One *8*, e62765. https://doi.org/10.1371/journal.pone.0062765.

36. Ward, Y., Lake, R., Yin, J.J., Heger, C.D., Raffeld, M., Goldsmith, P.K., Merino, M., and Kelly, K. (2011). LPA Receptor Heterodimerizes with CD97 to Amplify LPA-Initiated RHO-Dependent Signaling and Invasion in Prostate Cancer Cells. Cancer Res. *71*, 7301–7311. https://doi.org/10.1158/0008-5472.CAN-11-2381.

37. Wobus, M., Bornhäuser, M., Jacobi, A., Kräter, M., Otto, O., Ortlepp, C., Guck, J., Ehninger, G., Thiede, C., and Oelschlägel, U. (2015). Association of the EGF-TM7 receptor CD97 expression with FLT3-ITD in acute myeloid leukemia. Oncotarget *6*, 38804–38815. https://doi.org/10.18632/oncotarget.5661.

38. Ho, T.-C., LaMere, M., Stevens, B.M., Ashton, J.M., Myers, J.R., O'Dwyer, K.M., Liesveld, J.L., Mendler, J.H., Guzman, M., Morrissette, J.D., et al. (2016). Evolution of acute myelogenous leukemia stem cell properties after treatment and progression. Blood *128*, 1671–1678. https://doi.org/10.1182/blood-2016-02-695312.

39. Saito, Y., Kitamura, H., Hijikata, A., Tomizawa-Murasawa, M., Tanaka, S., Takagi, S., Uchida, N., Suzuki, N., Sone, A., Najima, Y., et al. (2010). Identification of Therapeutic Targets for Quiescent, Chemotherapy-Resistant Human Leukemia Stem Cells. Sci. Transl. Med. *2*, 17ra9. https://doi.org/10.1126/scitranslmed.3000349.

40. Martin, G.H., Roy, N., Chakraborty, S., Desrichard, A., Chung, S.S., Woolthuis, C.M., Hu, W., Berezniuk, I., Garrett-Bakelman, F.E., Hamann, J., et al. (2019). CD97 is a critical regulator of acute myeloid leukemia stem cell function. J. Exp. Med. *216*, 2362–2377. https://doi.org/10.1084/jem.20190598.

41. Vaikari, V.P., Yang, J., Wu, S., and Alachkar, H. (2019). CD97 expression is associated with poor overall survival in acute myeloid leukemia. Exp. Hematol. *75*, 64–73.e4. https://doi.org/10.1016/j.exphem.2019.06.474.

42. Tang, Z., Kang, B., Li, C., Chen, T., and Zhang, Z. (2019). GEPIA2: an enhanced web server for large-scale expression profiling and interactive analysis. Nucleic Acids Res. *47*, W556–W560. https://doi.org/10.1093/nar/gkz430.

43. Edgar, R., Domrachev, M., and Lash, A.E. (2002). Gene Expression Omnibus: NCBI gene expression and hybridization array data repository. Nucleic Acids Res. *30*, 207–210. https://doi.org/10.1093/nar/30.1.207.

44. Bagger, F.O., Kinalis, S., and Rapin, N. (2019). BloodSpot: a database of healthy and malignant haematopoiesis updated with purified and single cell mRNA sequencing profiles. Nucleic Acids Res. *47*, D881–D885. https://doi.org/10.1093/nar/gky1076.

45. Hsu, P.D., Scott, D.A., Weinstein, J.A., Ran, F.A., Konermann, S., Agarwala, V., Li, Y., Fine, E.J., Wu, X., Shalem, O., et al. (2013). DNA targeting specificity of RNA-guided Cas9 nucleases. Nat. Biotechnol. *31*, 827–832. https://doi.org/10.1038/nbt.2647.

46. Schumann, K., Lin, S., Boyer, E., Simeonov, D.R., Subramaniam, M., Gate, R.E., Haliburton, G.E., Ye, C.J., Bluestone, J.A., Doudna, J.A., and Marson, A. (2015). Generation of knock-in primary human T cells using Cas9 ribonucleoproteins. Proc. Natl. Acad. Sci. USA *112*, 10437–10442. https://doi.org/10.1073/pnas.1512503112.

47. Eyquem, J., Mansilla-Soto, J., Giavridis, T., van der Stegen, S.J.C., Hamieh, M., Cunanan, K.M., Odak, A., Gönen, M., and Sadelain, M. (2017). Targeting a CAR to the TRAC locus with CRISPR/Cas9 enhances tumour rejection. Nature *543*, 113–117. https://doi.org/10.1038/nature21405.

48. Jiang, J., Chen, J., Liao, C., Duan, Y., Wang, Y., Shang, K., Huang, Y., Tang, Y., Gao, X., Gu, Y., and Sun, J. (2023). Inserting EF1α-driven CD7-specific CAR at CD7 locus reduces fratricide and enhances tumor rejection. Leukemia *37*, 1660–1670. https://doi.org/10.1038/s41375-023-01948-3.

49. Liao, C., Wang, Y., Huang, Y., Duan, Y., Liang, Y., Chen, J., Jiang, J., Shang, K., Zhou, C., Gu, Y., et al. (2023). CD38-Specific CAR Integrated into CD38 Locus Driven by Different Promoters Causes Distinct Antitumor Activities of T and NK Cells. Adv. Sci. *10*, 2207394. https://doi.org/10.1002/advs.202207394.

50. Cappell, K.M., and Kochenderfer, J.N. (2021). A comparison of chimeric antigen receptors containing CD28 versus 4-1BB costimulatory domains. Nat. Rev. Clin. Oncol. *18*, 715–727. https://doi.org/10.1038/s41571-021-00530-z.

51. Feucht, J., Sun, J., Eyquem, J., Ho, Y.-J., Zhao, Z., Leibold, J., Dobrin, A., Cabriolu, A., Hamieh, M., and Sadelain, M. (2019). Calibration of CAR activation potential directs alternative T cell fates and therapeutic potency. Nat. Med. *25*, 82–88. https://doi.org/10.1038/s41591-018-0290-5.

52. Duan, Y., Chen, J., Meng, X., Liu, L., Shang, K., Wu, X., Wang, Y., Huang, Z., Liu, H., Huang, Y., et al. (2023). Balancing activation and co-stimulation of CAR tunes signaling dynamics and enhances therapeutic potency. Mol. Ther. *31*, 35–47. https://doi.org/10.1016/j.ymthe.2022.08.018.

53. Esther, S., Thomas, P., Ibrahim, E.-S., Ying, Z., Rui, H., Alina, M., Johan, H., Moustapha, H., Isabelle, M., and Jonas, M. (2023). Tuned activation of MSLN-CAR T cells induces superior antitumor responses in ovarian cancer models. Journal for ImmunoTherapy of Cancer *11*, e005691. https://doi.org/10.1136/jitc-2022-005691.

54. Skopek, R., Palusińska, M., Kaczor-Keller, K., Pingwara, R., Papierniak-Wygładała, A., Schenk, T., Lewicki, S., Zelent, A., and Szymański, Ł. (2023). Choosing the Right Cell Line for Acute Myeloid Leukemia (AML) Research. Int. J. Mol. Sci. *24*, 5377. https://doi.org/10.3390/ijms24065377.

55. Perna, F., Berman, S.H., Soni, R.K., Mansilla-Soto, J., Eyquem, J., Hamieh, M., Hendrickson, R.C., Brennan, C.W., and Sadelain, M. (2017). Integrating Proteomics and Transcriptomics for Systematic Combinatorial Chimeric Antigen Receptor Therapy of AML. Cancer Cell *32*, 506–519.e5. https://doi.org/10.1016/j.ccell.2017.09.004.

56. Gottschlich, A., Thomas, M., Grünmeier, R., Lesch, S., Rohrbacher, L., Igl, V., Briukhovetska, D., Benmebarek, M.-R., Vick, B., Dede, S., et al. (2023). Single-cell transcriptomic atlas-guided development of CAR-T cells for the treatment of acute myeloid leukemia. Nat. Biotechnol. *41*, 1618–1632. https://doi.org/10.1038/s41587-023-01684-0.

57. Hilbig, D., Sittig, D., Hoffmann, F., Rothemund, S., Warmt, E., Quaas, M., Stürmer, J., Seiler, L., Liebscher, I., Hoang, N.A., et al. (2018). Mechano-Dependent Phosphorylation of the PDZ-Binding Motif of CD97/ADGRE5 Modulates Cellular Detachment. Cell Rep. *24*, 1986–1995. https://doi.org/10.1016/j.celrep.2018.07.071.

58. Vizurraga, A., Adhikari, R., Yeung, J., Yu, M., and Tall, G.G. (2020). Mechanisms of adhesion G protein–coupled receptor activation. J. Biol. Chem. *295*, 14065–14083. https://doi.org/10.1074/jbc.REV120.007423.

59. Wang, N., Qian, Y., Xia, R., Zhu, X., Xiong, Y., Zhang, A., Guo, C., and He, Y. (2023). Structural basis of CD97 activation and G-protein coupling. Cell Chem. Biol. *30*, 1343–1353.e5. https://doi.org/10.1016/j.chembiol.2023.08.003.

60. Mao, C., Zhao, R.-J., Dong, Y.-J., Gao, M., Chen, L.-N., Zhang, C., Xiao, P., Guo, J., Qin, J., Shen, D.-D., et al. (2024). Conformational transitions and activation of the adhesion receptor CD97. Mol. Cell *84*, 570–583.e7. https://doi.org/10.1016/j.molcel.2023.12.020.

61. Ravn-Boess, N., Roy, N., Hattori, T., Bready, D., Donaldson, H., Lawson, C., Lapierre, C., Korman, A., Rodrick, T., Liu, E., et al. (2023). The

expression profile and tumorigenic mechanisms of CD97 (ADGRE5) in glioblastoma render it a targetable vulnerability. Cell Rep. *42*, 113374. https://doi.org/10.1016/j.celrep.2023.113374.

62. Vetrie, D., Helgason, G.V., and Copland, M. (2020). The leukaemia stem cell: similarities, differences and clinical prospects in CML and AML. Nat. Rev. Cancer *20*, 158–173. https://doi.org/10.1038/s41568-019-0230-9.

63. Liu, Y., Wu, W., Cai, C., Zhang, H., Shen, H., and Han, Y. (2023). Patient-derived xenograft models in cancer therapy: technologies and applications. Signal Transduct. Target. Ther. *8*, 160. https://doi.org/10.1038/s41392-023-01419-2.

64. Pei, S., Shelton, I.T., Gillen, A.E., Stevens, B.M., Gasparetto, M., Wang, Y., Liu, L., Liu, J., Brunetti, T.M., Engel, K., et al. (2023). A Novel Type of Monocytic Leukemia Stem Cell Revealed by the Clinical Use of Venetoclax-Based Therapy. Cancer Discov. *13*, 2032–2049. https://doi.org/10.1158/2159-8290.CD-22-1297.

65. Jing, R., Jiao, P., Chen, J., Meng, X., Wu, X., Duan, Y., Shang, K., Qian, L., Huang, Y., Liu, J., et al. (2021). Cas9-Cleavage Sequences in Size-Reduced Plasmids Enhance Nonviral Genome Targeting of CARs in Primary Human T Cells. Small Methods *5*, 2100071. https://doi.org/10.1002/smtd.202100071.

66. Kim, D., Langmead, B., and Salzberg, S.L. (2015). HISAT: a fast spliced aligner with low memory requirements. Nat. Methods *12*, 357–360. https://doi.org/10.1038/nmeth.3317.

67. Li, H., Handsaker, B., Wysoker, A., Fennell, T., Ruan, J., Homer, N., Marth, G., Abecasis, G., and Durbin, R.; 1000 Genome Project Data Processing Subgroup (2009). The Sequence Alignment/Map format and SAMtools. Bioinformatics *25*, 2078–2079. https://doi.org/10.1093/bioinformatics/btp352.

68. Liao, Y., Smyth, G.K., and Shi, W. (2014). featureCounts: an efficient general purpose program for assigning sequence reads to genomic features. Bioinformatics *30*, 923–930. https://doi.org/10.1093/bioinformatics/btt656.

69. Robinson, M.D., McCarthy, D.J., and Smyth, G.K. (2010). edgeR: a Bioconductor package for differential expression analysis of digital gene expression data. Bioinformatics *26*, 139–140. https://doi.org/10.1093/bioinformatics/btp616.

70. Wu, T., Hu, E., Xu, S., Chen, M., Guo, P., Dai, Z., Feng, T., Zhou, L., Tang, W., Zhan, L., et al. (2021). clusterProfiler 4.0: A universal enrichment tool for interpreting omics data. Innovation *2*, 100141. https://doi.org/10.1016/j.xinn.2021.100141.

71. Subramanian, A., Tamayo, P., Mootha, V.K., Mukherjee, S., Ebert, B.L., Gillette, M.A., Paulovich, A., Pomeroy, S.L., Golub, T.R., Lander, E.S., and Mesirov, J.P. (2005). Gene set enrichment analysis: A knowledge-based approach for interpreting genome-wide expression profiles. Proc. Natl. Acad. Sci. USA *102*, 15545–15550. https://doi.org/10.1073/pnas.0506580102.

Please cite this article in press as: Shang et al., CD97-directed CAR-T cells with enhanced persistence eradicate acute myeloid leukemia in diverse xenograft models, Cell Reports Medicine (2025), https://doi.org/10.1016/j.xcrm.2025.102148

STAR★METHODS

KEY RESOURCES TABLE

REAGENT or RESOURCE	SOURCE	IDENTIFIER
Antibodies		
Human CD3 (UCHT1, APC-eFluor™780)	Thermo Fisher Scientific	Cat# 47-0038-42; RRID: AB_1272042
Human CD45RA (HI100, eFluor™506)	Thermo Fisher Scientific	Cat# 69-0458-41; RRID: AB_2637379
Human CD62L (DREG-56, eFluor™450)	Thermo Fisher Scientific	Cat# 48-0629-42; RRID: AB_10853514
Human CD223 (LAG-3) (3DS223H, PerCP- eFluor™710)	Thermo Fisher Scientific	Cat# 46-2239-42; RRID: AB_2573732
Human CD33 (WM53, BV421)	BD Biosciences	Cat# 562854; RRID: AB_2737405
Human CD34 (581, BV421)	BD Biosciences	Cat# 562577; RRID: AB_2687922
Human CD36 (CB38, APC)	BD Biosciences	Cat# 550956; RRID: AB_398480
Human CD4 (SK3, BV711)	BD Biosciences	Cat# 563028; RRID: AB_2737961
Human CD4 (SK3, BUV395)	BD Biosciences	Cat# 563550; RRID: AB_2738273
Human CD45 (HI30, Alexa Fluor® 700)	BD Biosciences	Cat# 560566; RRID: AB_1645452
Human CD64 (10.1, BV510)	BD Biosciences	Cat# 563459; RRID: AB_2738220
Human CD8 (SK1, APC-Cy7)	BD Biosciences	Cat# 557834; RRID: AB_396892
Human CD8 (SK1, BV605)	BD Biosciences	Cat# 564116; RRID: AB_2869551
Human CD11b (ICRF44, PE)	BD Biosciences	Cat# 555388; RRID: AB_395789
Human CD97 (VIM3b, PE)	BD Biosciences	Cat# 555774; RRID: AB_396110
Human CD279 (PD-1) (EH12.1, BV510)	BD Biosciences	Cat# 563076; RRID: AB_2737990
Human CD366 (TIM-3) (7D3, BV421)	BD Biosciences	Cat# 565562; RRID: AB_2744369
Mouse IgG1, κ isotype control antibody (MOPC-21, PE)	BioLegend	Cat# 400113; RRID: AB_326435
Mouse CD16/CD32 (93)	BioLegend	Cat# 101302; RRID: AB_312801
Human CD85k (ILT3) (ZM4.1, PE-Cyaine7)	BioLegend	Cat# 333011; RRID: AB_2564066
Human CD117 (c-kit) (104D2, BV605)	BioLegend	Cat# 313218; RRID: AB_2562025
Human CD97 polyclonal antibody	ABclonal	Cat# A3780; RRID: AB_2765268
Anti-GADPH mouse monoclonal antibody	Proteintech	Cat# 60004-1-Ig; RRID: AB_2107436
Biological samples		
Healthy donor peripheral blood, fresh	Zhejiang University	N/A
Healthy donor peripheral blood, mobilizing agents treated	The First Affiliated Hospital, Zhejiang University	N/A
AML patient samples	The First Affiliated Hospital, Zhejiang University	N/A
Umbilical cord blood	Zhejiang Cord Blood Bank	N/A
Chemicals, peptides, and recombinant proteins		
Cas9 protein	This paper	N/A
Recombinant Human IL-7	Novoprotein	Cat# GMP-CD47
Recombinant Human IL-15	Novoprotein	Cat# GMP-C016
RetroNectin	Takara	Cat# T100A
LIVE/DEAD Fixable Near-IR Dead Cell Stain Kit	Invitrogen	Cat# L10119
CountBright™ absolute counting beads	Invitrogen	Cat# C36950
CTS™ Dynabeads™ CD3/CD28	Gibco	Cat# 40203S
Critical commercial assays		
Pan T cell Isolation Kit, human	Miltenyi Biotec	Cat# 130-096-535
CD34 MicroBead Kit UltraPure, human	Miltenyi Biotec	Cat# 130-100-453
MethoCult H4034 Optimum	STEMCELL	Cat# 04034

(*Continued on next page*)

Continued

REAGENT or RESOURCE	SOURCE	IDENTIFIER
Deposited data		
AML samples with normal cells	BloodSpot (v2.0)	RRID: SCR_015563; Download: https://www.bloodspot.eu/
AML samples with normal cells	GEPIA2	RRID: SCR_018294; Download: http://gepia2.cancer-pku.cn
RNA-seq data	This paper	CNGB: CNP0007174
Experimental models: Cell lines		
HEK293T	ATCC	Cat# CRL-3216; RRID: CVCL_0063
KG-1	ATCC	Cat# CCL-246; RRID: CVCL_0374
Kasumi-1	ATCC	Cat# CRL-2724; RRID: CVCL_0589
NB4	DSMZ	Cat# ACC 207; RRID: CVCL_0005
HL-60	ATCC	Cat# CCL-240; RRID: CVCL_0002
OCI-AML2	DSMZ	Cat# ACC 99; RRID: CVCL_1619
OCI-AML3	DSMZ	Cat# ACC 582; RRID: CVCL_1844
MOLM-13	DSMZ	Cat# ACC 554; RRID: CVCL_2119
THP-1	ATCC	Cat# TIB-202; RRID: CVCL_0006
U937	ATCC	Cat# CRL-1593.2; RRID: CVCL_0007
Experimental models: Organisms/strains		
NSG mouse: NOD.Cg-*Prkdc*^{scid} *Il2rg*^{em1Smoc} (M-NSG)	Shanghai Model Organisms Center	Cat# NM-NSG-001; RRID: IMSR_NM-NSG-001
NSG mouse: NOD.Cg-*Prkdc*^{scid}*Il2rg*^{tm1Wjl}Tg (CMV-IL3,CSF2,KITLG)1Eav/MloySzJ (NSG-S)	The Jackson Laboratory	Cat# 013062; RRID: IMSR_JAX:013062
Oligonucleotides		
TRAC sgRNA target sequence: 5′-CAGGGTTCTGGATATCTGT	GenScript	N/A
CD97 sgRNA target sequence: 5′-TCTGAGCCACAACAACACCA	GenScipt	N/A
Recombinant DNA		
pSFG-aCD97-HL-P2A-EGFP	This paper	N/A
pSFG-aCD97-LH-P2A-EGFP	This paper	N/A
pAAV-aCD97-28z-T2A-EGFP	This paper	N/A
pAAV-aCD97-28z-1XX-T2A-EGFP	This paper	N/A
pAAV-aCD97-BBz-T2A-EGFP	This paper	N/A
Software and algorithms		
GraphPad Prism v9.5.1	GraphPad Software	N/A
FlowJo v10.8.1	BD Biosciences	N/A
GESA_4.3.2	UC San Diego and Broad Institute	N/A

EXPERIMENTAL MODEL AND STUDY PARTICIPANT DETAILS

AML patient samples

All primary samples were obtained from The First Affiliated Hospital, Zhejiang University School of Medicine, after informed consent and approval by the institutional medical ethical committee (2022-093). Bone marrow samples were obtained from AML patients through bone marrow aspiration and mononuclear cells were isolated through density gradient centrifugation. Primary cells were cultured in StemSpan SFEM II with 50 ng/mL SCF, 10 ng/mL TPO, 10 ng/mL FLT-3L, 10 ng/mL IL-3 and 10 ng/mL IL-6. The detail information of each patient was shown in the Table S1.

Cell lines

293T cells were maintained in Dulbecco's modified Eagle's medium (DMEM) (Gibco) supplemented with 10% fetal bovine serum (FBS) (Excell Bio) containing 1% penicillin/streptomycin (Gibco). For AML cell lines, HL-60 cells were cultured in Iscove's modified Dulbecco's medium (IMDM) with 20% FBS and 1% penicillin/streptomycin. OCI-AML2 and OCI-AML3 cells were cultured in

minimum essential medium (MEM) α (Gibco) with 20% FBS and 1% penicillin/streptomycin. KG-1, Kasumi-1, NB4, MOLM-13, THP-1 and U937 were all cultured in RPMI1640 (BasalMedia) with 10% FBS and 1% penicillin/streptomycin.

In vivo models

For cell line-derived xenograft models, 6-10 weeks-old NOD.Cg-*Prkdc*^{scid}*Il2rg*^{em1Smoc} (M-NSG) mice were purchased from Shanghai Model Organisms Center and maintained at the Laboratory Animal Center, Zhejiang University. All the procedures were approved by the ethical committee of Zhejiang University (20220178). Mice were inoculated with 1×10^6 HL-60-FFLuc-mCherry, OCI-AML2-FFLuc-mCherry or MOLM-13-FFLuc-mCherry cells by tail vein injection. CAR-T cells were injected in the same way 4 or 7 days later. To measure luminescence, mice were injected with D-luciferin intraperitoneally. Tumor burden was monitored by a Biospace Optima small animal imaging system (Biospace Lab) or IVIS imaging system (PerkinElmer), and M3 vision software (Biospace Lab) or Living Image software (PerkinElmer) was used to visualize and calculate luminescence.

For patient-derived xenograft models, both AML patient samples were obtained as donations with written informed consent and with the approval of the local human subject research ethics board at The First Affiliated Hospital of Zhejiang University. The use of the patient-derived primary AML cells was reviewed and approved by the Clinical Research Ethics Committee of the First Affiliated Hospital, Zhejiang University School of Medicine (IIT20240068B). Primary human AML specimens were obtained from leukapheresis product. As previously described,[64] NOD.Cg-*Prkdc*^{scid}*Il2rg*^{tm1Wjl}Tg (CMV-IL3, CSF2, KITLG) 1Eav/MloySzJ (NSG-S) mice were used in this study. Female mice ranging in age from 6 to 8 weeks were started on the experiment. Littermates were randomly assigned to experimental groups. NSG-S mice were preconditioned 24 h prior to transplant with 30 mg/kg busulfan via intraperitoneal injection. For primary transplantation, 5×10^6 cells were transplanted via tail vein injection. For secondary transplantation used to compare LSC activity from primary transplants receiving control or CAR-T therapy, total bone marrow from equal number of primary transplanted mice from both groups were harvested side by side. The cells from the CAR-T treated group were then flow sorted to remove EGFP$^+$ CAR-T cells. After sorting of the CAR-T group, all cells from both groups were resuspended in equal volume and injected into same number of secondary NSG-S recipients.

METHOD DETAILS

CAR design and construction

The scFv V_H and V_L sequences were derived from a murine CD97-specific antibody (CN110627903) and then synthesized commercially (GenScript). For the retroviral system, the scFvs (V_H-V_L or V_L-V_H) replaced the original scFv of the SFG γ-retroviral vector containing a second-generation 1928z CAR sequence.[47,51] An EGFP gene was added after a P2A peptide sequence as a reporter for CAR expression. For the AAV system, 9728z, 9728z-1XX or 97BBz CARs were cloned into a pAAV vector[47,51] separately and EGFP was inserted after CAR via a T2A peptide sequence to detect the CAR expression.

Isolation and expansion of human T cells

Peripheral blood was obtained from healthy volunteers who provided informed consent. Ethical permission was granted by the School of Medicine, Zhejiang University (2020-067). All blood samples were handled following the required ethical and safety procedures. Peripheral blood mononuclear cells (PBMCs) were isolated from the peripheral blood by Ficoll density gradient centrifugation (Dakewe). T cells were isolated from PBMCs using Pan T cell Isolation kit (Miltenyi Biotec) and then stimulated with CD3/CD28 T cell Activator Dynabeads (Gibco) for 48 h. X-VIVO 15 Serum-free Hematopoietic Cell medium (Lonza) with 10% FBS, 1% penicillin/streptomycin, 5 ng/mL interleukin-7 (IL-7) and 5 ng/mL interleukin-15 (IL-15) (Novoprotein) was used for T cell cultivation.

gRNA sequence

TRAC gRNA sequence: 5′-mC*mA*mG*GGUUCUGGAUAUCUGUGUUUUAGAGCUAGAAAUAGCAAGUUAAAAUAAGGCUAGUCCGUUAUCAACUUGAAAAAGUGGCACCGAGUCGGUGCU*mU*mU*mU-3′

CD97 gRNA sequence: 5′-mU*mC*mU*GAGCCACAACAACACCAGUUUUAGAGCUAGAAAUAGCAAGUUAAAAUAAGGCUAGUCCGUUAUCAACUUGAAAAAGUGGCACCGAGUCGGUGCU*mU*mU*mU-3′

m represents 2′-*O*-methyl RNA and asterisk (*) represents phosphorothioate.

CAR-T cell production and gene targeting

To generate CD97-HL and CD97-LH CAR-T cells, retroviruses were produced by 293T cells. The anti-CD3/CD28 beads were used to initiate T cell activation and removed magnetically after 48 h. T cells were transduced with retroviral supernatant by centrifugation on retronectin (Takara)-coated plates. 24 h after transduction, cells were changed into fresh complete medium. To generate *CD97*^{KO}-9728z, *CD97*^{KO}-9728z-1XX and *CD97*^{KO}-97BBz CAR-T cells, 1×10^6 T cells were mixed with ribonucleoproteins (RNPs), which were formed by mixing 60 pmol gRNA and 6 μg Cas9 in a total volume of 20 μL. Modified gRNAs were synthesized by GeneScript and Cas9 proteins were produced as described in the previous work.[65] After being transferred to a 20 μL cuvette, electroporation was performed by a cell electroporator (CELETRIX). Cells were then transferred into culture medium and AAV virus (Vigene Biosciences, MOI = 2.5×10^5) was added 20 min later.

Cell viability and cell number assay

A mixture of acridine orange (AO) and propidium iodide (PI) was used to stain viable and dead cells. Cell number and viability were analyzed by a Countstar Rigel S3 Fluorescence Cell Analyzer (Countstar).

AML cell line cytotoxicity assay

The HL-60 cells, OCI-AML2 cells, OCI-AML3 cells and MOLM-13 cells were transduced to express FFLuc and sorted by mCherry. For luciferase-based cytotoxicity assay, the effector (E) and target (T) cells were co-cultured in triplicates at indicated E/T ratios using black 96-well flat plates (WHB) with 5×10^4 target cells in a total volume of 100 μL per well. Target cells alone were also plated at the same cell density to determine the maximal luciferase expression (relative light units, RLU). 18 h later, 100 μL of 1.5 mg/mL luciferase substrate (Perkin) was directly added to each well. Emitted light was detected in Varioskan Flash (Thermo Fisher Scientific). Lysis was determined as $[(RLU_{max} - RLU_{sample})/RLU_{max}] \times 100\%$. If the value was negative, it was identified as zero. Unless specification, all CAR-T cells have not undergone sorting for pure CAR positive cells. Instead, a mixed population was utilized for this and following experiments.

Primary AML cells and HSPCs cytotoxicity assay

To evaluate the cytotoxicity on primary AML cells or HSPCs by CAR-T cells, primary AML cells or HSPCs were labeled with CytoTell Red (AAT Bioquest) to distinguish primary tumor cells or HSPCs from CAR-T cells. Labeled cells were co-cultured with CAR-T cells or UTD T cells at a ratio of 2:1 or 1:1 for 24 h in triplicate. All the cells were collected for flow cytometry. Dead cells were indicated by DAPI staining and absolute cell counts of viable primary cells were quantified using CountBright Plus Absolute Counting Beads (Invitrogen). Lysis was determined as $[(Number_{Target\ only} - Number_{Target\ remain})/Number_{Target\ only}] \times 100\%$. $Number_{Target\ only}$ means the cell number of target cells without co-culturing. $Number_{Target\ remain}$ means the remaining cell number of target cells following co-culturing with CAR-T cells or UTD T cells.

Cytokine release measurement

To evaluate cytokine production ability, CAR-T cells were co-cultured with target cells at an E/T ratio of 4:1 for 24 h. Then, the cell culture supernatant was harvested and Cytometric Bead Arrays (CBA, BD Biosciences) for TNF-α and IFN-γ were used according to the manufacturer's instructions. In brief, a mixture of capture beads (TNF-α or IFN-γ) and cell supernatant was incubated for 1 h and then PE-detection reagent was added to incubate for another 2 h. Beads were washed and analyzed by flow cytometry.

Proliferation assay

For the proliferation assay, CAR-T cells were labeled with CytoTell Red according to the manufacturer's instructions. Briefly, cells were resuspended in pre-warmed D-PBS (KeyGEN BioTECH) at a final concentration of 1×10^6 cells/mL. Cell dye was added at the suggested working concentration. The CAR-T cells were incubated with cell dye at 37°C for 15 min and then washed three times with D-PBS. Labeled CAR-T cells were further stimulated with HL-60 cells in triplicates at a ratio of 4:1. Also, labeled CAR-T cells without stimulation were served as a control. After 72 h, cells were harvested and analyzed by flow cytometry.

Antigen stimulation and persistence assay

For weekly antigen stimulations, 5×10^5 CAR-T cells were co-cultured with AML cells (HL-60, OCI-AML2 or MOLM-13) at a ratio of 4:1 in 24-well plate. Total cells were counted and CAR expression as well as PD-1 and LAG-3 expression were determined weekly by flow cytometry. Subsequently, CAR-T cells were restimulated under the same conditions.

Colony formation assay

Normal HSPCs were isolated from the umbilical cord blood of healthy donors using CD34 specific microbeads (Miltenyi Biotec). Bone marrow derived HSPCs were isolated from the peripheral blood of a healthy donor treated with mobilizing agents via the same microbeads. After separation, 1×10^3 HSPCs were incubated with UTD or CAR-T cells, or medium at an E/T ratio of 1:1 for 4 h. Medium was StemSpan SFEM II with 50 ng/mL SCF, 10 ng/mL TPO, 10 ng/mL FLT-3L, 10 ng/mL IL-3 and 10 ng/mL IL-6. After incubation, the cell suspension was transferred to a methyl cellulose-based medium (MethoCult H4034 Optimum, STEMCELL) in triplicate. After 14 days, CFU-E, BFU-E, CFU-G/M and CFU-GEMM colonies were counted.

Immunoblotting assay

The cells were lysed in RIPA buffer (Beyotime) containing protease inhibitor cocktail (Yeasen) by ultrasonic cell disruptor (XinZhi). The protein concentration of cell lysates was determined with the Enhanced BCA Protein Assay Kit (Beyotime) according to the manufacturer's instructions. The samples were boiled with 5×SDS loading buffer at 95°C for 10 min. For the immunoblotting assay, 30 μg proteins were separated by SDS-PAGE and transferred onto a PVDF membrane (Bio-Rad). The membrane was blocked using 5% bovine serum albumin (BSA, Sangon Biotech) in TBS-T (Tris-buffer saline containing 0.05% Tween 20) buffer for 1 h at room temperature. The membrane was then probed with Rabbit anti-human CD97 polyclonal antibody (ABclonal) and Mouse anti-human GADPH monoclonal antibody (Proteintech) overnight at 4°C. After washing with TBS-T three times (10 min each), the membrane was probed

with horseradish peroxidase (HRP)-conjugated antibody to rabbit IgG (Proteintech) or mouse IgG (Proteintech) for 1 h at room temperature. The membrane was visualized with standard chemiluminescence (CLINX).

Flow cytometry

All flow cytometry experiments were performed using standard sample processing and staining protocols. Assays were performed on CytoFLEX (Beckman Coulter), CytoFLEX LX (Beckman Coulter), Attune (Thermo Fisher Scientific) or BD LSRFortessa (BD Biosciences). MoFlo Astrios EQ (Beckman Coulter) was used for cell sorting. CAR transgene positive T cells were identified by detection of EGFP. Live cells were identified as staining negative for DAPI (Yeasen) or LIVE/DEAD Fixable NIR Dead Cell Stain Kit (Thermo Fisher Scientific). Raw data were analyzed with the FlowJo software v.10.8.1. High-dimensional data analysis using dimensionality reduction and automated clustering of concatenated samples were performed in FlowJo via its native platform for running t-distributed stochastic neighbor embedding.

Isolation of cells from bone marrow, spleen and blood

To analyze the immunophenotype of CAR-T cells, mice were sacrificed at day 41 after CAR-T cells administration. Bone marrow cells were harvested from freshly isolated femurs and tibias. After removal of connective tissues and muscles, bones and spleens were crushed in 5 mL PBS with 0.25% BSA. Single-cell suspensions were made by pipetting and passing supernatant through a 40 μm filter. Blood was collected from the submandibular vein. Red blood cells were lysed by ACK buffer (Solarbio) before further usage.

Leukemia burden and immunophenotyping

As previous described,[64] peripheral blood and/or bone marrow samples of PDX mice were stained with flow panels to evaluate leukemia burden and immunophenotype. The leukemia burden flow panel contains antibodies against human CD33 (BD Horizon; cat. # 562854), CD8 (BD Horizon; cat. # 564116), CD4 (BD Horizon; cat. # 563028), CD97 (BD Pharmingen; cat. # 555774) and CD45 (BD Pharmingen; cat. # 560566). The immunophenotyping panel contains antibodies against human CD34 (BD Horizon; cat. # 562577), CD64 (BD Horizon; cat. # 563459), CD117 (BioLegend; cat. # 313218), CD4 (BD Horizon; cat. # 563028), CD11b (BD Pharmingen; cat. # 555388), CD85k (BioLegend; cat. # 333011), CD36 (BD Pharmingen; cat. # 550956) and CD45 (BD Pharmingen; cat. # 560566). All samples were stained in room temperature for 15 min, washed with ice-cold FACS buffer, and resuspended in FACS buffer containing LIVE/DEAD Fixable Near-IR Dead Cell Stain Kit (Thermo Fisher, cat. #L10119) and counting beads (Thermo Fisher, cat. #C36950), analyzed on a Attune flow cytometer (Thermo Fisher).

RNA extraction, transcriptome sequencing and RNA-seq analysis

CD97^{KO}-9728z and *CD97*^{KO}-9728z-1XX CAR-T cells were stimulated with HL-60 cells every 24 h for thrice, followed by FACS selection of CAR positive (EGFP positive) cells. Total RNA was isolated with Trizol, and then first-strand cDNA synthesis and cDNA libraries were constructed using the NEBNext UltraTM II RNA Library Prep Kit (New England Biolabs). cDNA quality was determined on Agilent 2100 BioAnalyzer (Agilent Technologies), and then sequenced on NovaSeq 6000 device (Illumina) to obtain pair-end 150 bp reads.

Raw data was trimmed by Trim Galore (v0.6.10). Clean data were aligned to the Homo sapiens reference genome GRCh38 by HISAT2 (v2.1.0)[66] with default setting. The resulting SAM files were converted to sorted BAM files using SAMtools (version 1.7).[67] The aligned reads were quantified at the gene level using featureCounts (version 2.0.1).[68]

Differentially expressed genes (DEGs) were defined with a log2 fold change cutoff of |1| and a false discovery rate (FDR) < 0.05 by edgeR (v3.40.0).[69] Significant DEGs were analyzed for Gene Ontology (GO) enrichment using the clusterProfiler package (version 4.8.1).[70] Volcano plots were created using the EnhancedVolcano R package (https://github.com/kevinblighe/EnhancedVolcano). GSEA was performed using GSEA software (Broad Institute, v4.3.2)[71] with gene sets from GO knowledgebase and KEGG database related to T cell functions.

QUANTIFICATION AND STATISTICAL ANALYSIS

Statistical analysis

Prism 9 (GraphPad Software) was used for statistical analysis. For comparisons between two groups, we used the two-tailed Student's t test. For three or more groups, one-way or two-way analysis of variance (ANOVA) was used. We used linear regression analysis to assess correlation between CD97 expression on target cells and CAR-T cell mediated cytotoxicity. The survival was analyzed using a Mantel-Cox log-rank test. Values of $p < 0.05$ were considered statistically significant.